
Electronic Journal of
SEVERE STORMS METEOROLOGY

Topographic Sensitivity of the Snake River Plain Convergence Zone of Eastern Idaho. Part II: Numerical Simulations

THOMAS A. ANDRETTA

Department of Atmospheric Science, University of Wyoming, Laramie, Wyoming
(Submitted 10 March 2013; in final form 21 January 2014)

ABSTRACT

The Snake River Plain Convergence Zone (SPCZ) is a mesoscale topographic weather system in the planetary boundary layer that occasionally forms in a post-cold-frontal environment during the cold season in eastern Idaho. Part I of this study investigated persistent and locally heavy topographic snowfall associated with such a zone on 26 November 2005. Multiple snowbands formed in the presence of conditional, convective, and inertial instabilities. In Part II, nested grid high-resolution numerical simulations of the WRF-ARW model are used to investigate the structure and evolution of the SPCZ with two different terrain grid scales. In a smoothed topography with a coarsely resolved tributary valley system upstream of the broad parabolic-shaped Snake Plain, the model does not simulate a lee convergence band and vorticity dipole. These features are evident in the observations and control simulation. The smoothed run also misses snowfall associated with windward convergence and stable upslope flow in the Pocatello-Inkom area. Nevertheless, both model runs depict topographically-generated convective storms and potential vorticity anomalies in the plain.

1. Introduction

The Snake River Plain Convergence Zone (SPCZ) is a planetary boundary layer mesoscale topographic weather system that occasionally forms in a post-cold-frontal environment during the cold season in eastern Idaho (Andretta 2011). The zone has been documented in individual events with *in situ* and remote observations (Andretta and Hazen 1998) and in terms of a multi-year antecedent synoptic climatology (Andretta 2002; Andretta 2011). Andretta and Geerts (2010) used satellite, surface, radar, and aircraft data to study the meso- β -scale (20–200 km) structure of a persistent autumn SPCZ event in November 2005. The surface observations recorded snowfall accumulations of 25–38 cm (10–15 in) east and south of the city of Pocatello and revealed several well-defined snowbands in the radar reflectivity, a salient confluent pattern in the radial velocity winds, and alternating cyclonic and anticyclonic relative vertical vorticity structures.

These vorticity features, extending from the tributary valley-ridge systems in the Central Mountains to the Lower Snake River Plain, formed under weak to moderate low-level horizontal wind shear.

a. Motivation of study

This manuscript explores the dynamics of this SPCZ event with nested grid high-resolution numerical simulations. The principal motivation for this work is to understand the physical processes governing the evolution of terrain-induced convergence zones in eastern Idaho. This research hopefully will benefit the operational weather forecasting community.

An investigation of the physical processes within the SPCZ can be accomplished through the use of high-resolution numerical models, in which one or more variables is perturbed from a given initial state. Accordingly, this manuscript explores the evolution and structure of the SPCZ in the Weather Research and Forecasting (WRF)-Advanced Research WRF (ARW) (Skamarock et al. 2008) model using two topographic grid scales. An analysis of these distinct topographic grid scales is provided in a separate section of the paper.

Corresponding author address:

Thomas A. Andretta, Dept. of Atmospheric Science,
University of Wyoming, Laramie, WY 82071
E-mail: tandrett@uwyo.edu

Section 2 describes the region of study. Section 3 provides a definition of the SPCZ. Sections 4 and 5 outline the data sources and data processing, including the WRF-ARW model configuration and simulation experiments. Section 6 discusses the results of the numerical simulations of the 26 November 2005 SPCZ event with the different topographic grid scales.

b. Description of research questions

This study explores several research questions involving the evolution of the SPCZ in different topographic grid scales. This issue will be covered in

greater detail in section 4. The following research questions are addressed: How does the terrain grid scale affect the horizontal structure of the convergence bands, vorticity maxima and minima, and snowbands? Does the different terrain grid scales alter the convergence patterns, related circulations, and convection in the Snake Plain? How does the terrain grid scale modulate the potential vorticity anomalies within the reflectivity signatures of the SPCZ? These research questions are fully addressed in section 6 of the manuscript.

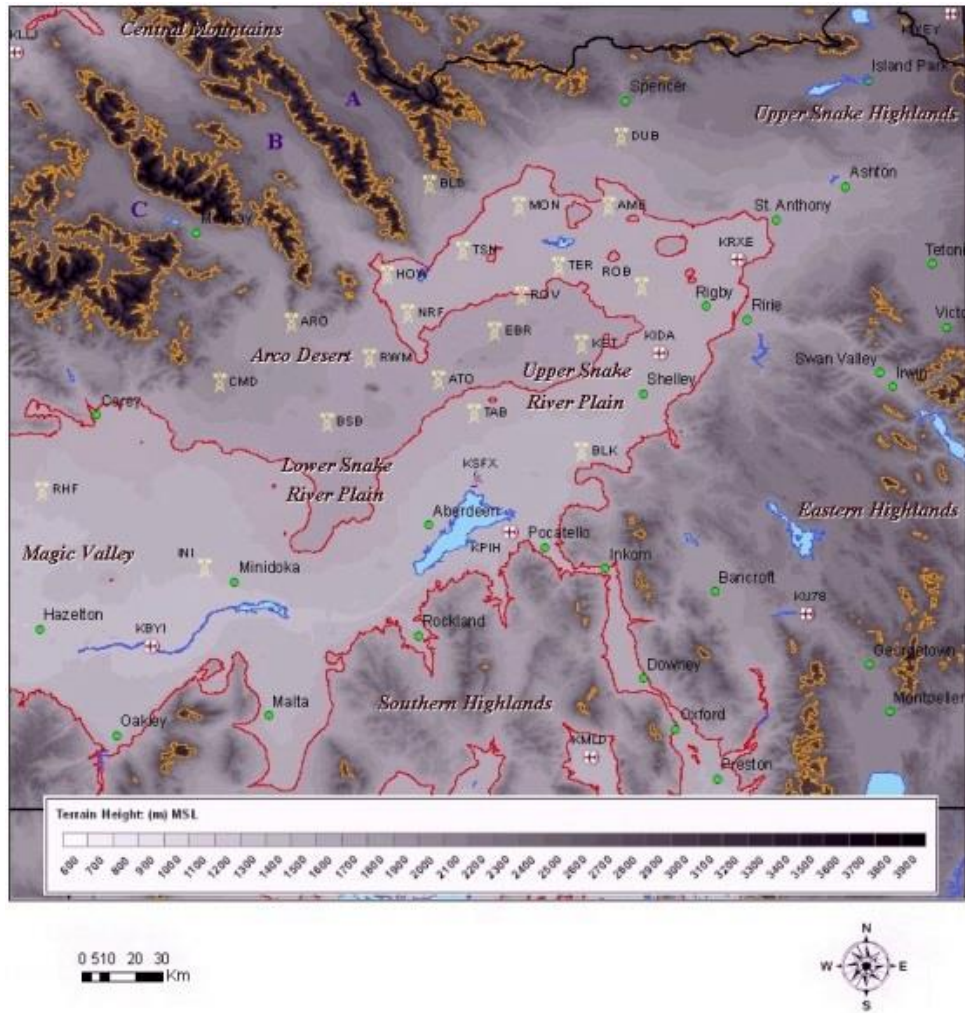


Figure 1: Eastern Idaho—USGS Digital Elevation Model (DEM) featuring 90-m data spacing (grey shades) with geographic regions (brown italic labels). The Birch Creek (A), Little Lost River (B), and Big Lost River (C) Valleys (purple labels) are labeled. The $z = 1500$ -m MSL (solid red contours) and $z = 2500$ -m MSL (solid orange contours) elevations illustrate the key topographic features in the text. Solid blue regions correspond to bodies of water. City names (filled green circles with black labels), Doppler weather radar facility (purple dish symbol: KSFX), and various station identifiers (yellow tower symbols with black labels) are indicated on the map (Andretta 2011).

2. Region of study

The geographical domain of eastern Idaho is illustrated in Fig. 1. The Snake River Plain is ~250 km long and ~100 km wide, curving around the Central Mountains from the west towards the northeast. The large plain includes the Magic Valley, the Lower Snake River Plain, and the Upper Snake River Plain. This enclosed wide plain gradually ascends from ~1000 m (all heights above MSL) at the western end of the Magic Valley to ~1700 m near the eastern end of the upper plain. The Upper Snake River Plain contains a shallow, fishhook-shaped topographic depression (1500 m red contour in Fig. 1). The Snake River Plain is circumscribed by several large mountain ranges: the Central Mountains (~2500–3000 m) to the northwest, the Eastern Highlands (~2500–3000 m) and Upper Snake Highlands (~2500–3000 m) to the east, and Southern Highlands (~2000–2500 m) to the south of the plain.

The city of Pocatello (1356 m) is located along one of the ranges of the Southern Highlands near an inflection point in the eastern part of the Snake River Plain. There are several narrow tributary valleys emptying from the Central Mountains onto the Arco Desert and Snake River Plain. The main canyons are named the Birch Creek (purple label A in Fig. 1), Little Lost River (B), and Big Lost River (C) valleys. These valleys and the contiguous Snake Plain are dry topographic features with climatological annual precipitation below 25 cm (10 in) (Andretta 2011). Consequently, significant precipitation events in the plain, like this SPCZ event (Andretta and Geerts 2010; Andretta 2011), represent a departure from the regional climatology and warrant closer examination by meteorologists.

3. Definition of SPCZ

The SPCZ can be defined in terms of the scales of atmospheric motion and physical forces (Andretta 2011). To further this understanding, it is helpful to identify these unitless scalar quantities: Rossby number (Ro) and Froude number (Fr). The Ro describes the departure of an atmospheric scale of motion from geostrophic wind balance (Holton 2004). It is expressed as $Ro = U/fL$, where U is the wind velocity ($m\ s^{-1}$), f is Coriolis parameter (s^{-1}), and L is scale of motion (m). Andretta (2011) found that the SPCZ occurs on a scale of atmospheric motion in the planetary boundary layer that departs from geostrophic wind balance ($Ro \approx 1.0$). The SPCZ is a mesoscale weather system. By comparison, a typical value of the Ro for mid-latitude synoptic-scale weather systems is $Ro \approx 0.1$ (Holton

2004). The Fr describes the ratio of the kinetic energy (approaching flow to a barrier) to the potential energy (vertical stability and obstacle height) (Mass and Ferber 1990; Reinecke and Durran 2008). This quantity is expressed as:

$$Fr = \frac{\overline{U}}{\overline{N} \times H} \quad (1)$$

where \overline{U} is the mean wind speed ($m\ s^{-1}$) below the (smoothed) highest terrain, \overline{N} is the mean Brunt-Väisälä frequency (s^{-1}) over the same depth, and H is the effective height (m) of the highest terrain over the mean height of the surrounding region.

The SPCZ forms under various physical forces. As Fig. 2 indicates, a low-level wind maximum (green arrows) induced by a zonal horizontal pressure gradient force becomes aligned with the long axis of the Magic Valley and intercepts the southern and eastern slopes of the Southern Highlands. This low-level wind is characterized by an ageostrophic flow of the first kind in which the horizontal pressure gradient force is greater than the Coriolis force (Haltiner and Martin 1957; Holton 2004). The pressure gradient force is given by $-\nabla p/\rho$, where ∇p is pressure gradient ($Pa\ m^{-1}$) and ρ is air density ($kg\ m^{-3}$). The Coriolis force is given by $-f\mathbf{k} \times \mathbf{V}$, where f is Coriolis parameter (s^{-1}), \mathbf{k} is the unit vector in the z-direction, and \mathbf{V} is wind velocity vector ($m\ s^{-1}$). Andretta (2011) discovered that the horizontal pressure gradient force is typically 2–4 times greater than the Coriolis force in some SPCZ cases. This flow is geostrophically unbalanced and does not result in a barrier jet (Parish 1982). Consequently, the flow creates upwind or windward convergence (scaloped white region in Fig. 2) along the gentle elevation rise in the eastern part of the Magic Valley and Lower Snake River Plain. The flow approaches the Southern Highlands but does not move over it and remains in the Magic Valley. This windward blocking by the Southern Highlands is characterized by low Fr ($0 < Fr < 1$). If there is sufficient moisture available and lifted by the topography, this stable flow generates precipitation in the lower plain near Pocatello and along the adjacent mountain ranges.

By comparison, the lower tropospheric static stability is high enough for obstacle flow that is diverted around the Central Mountains. Under this condition of stably stratified blocked flow, there is low Fr ($0 < Fr < 1$). As Fig. 2 illustrates, larger-scale low-level flow (blue arrows) moves past Boise Air

4. Data sources

a. Description of numerical experiments

This section describes the WRF-ARW model and sensitivity experiments. The high-resolution nonhydrostatic WRF-ARW (Skamarock et al. 2008) model is used to investigate the genesis and structure of the SPCZ. Table 1 lists the settings and details of the numerical simulations for the 26 November 2005 SPCZ event. The model domains (H1, H2, and H3) and topography at grid scales in the innermost nested grid (H3) are shown in Figs. 3 and 4, respectively.

There is two-way nesting between the outer model grid (H1) and inner model nested grids (H2) and (H3). Given the model grid interval of Δx , the smallest resolvable feature in the grid is $4 \Delta x$ (Grasso 2000). As Fig. 3 illustrates, this study features two numerical experiments corresponding to two different topographic grid scales (CONTROL and SMOOTH) in the model. The topography is the same (10 arcmin) for outer grid H1 in both simulations. However, the topographic grid scale for inner model grids H2 and H3 differs by factors of 5 and 20 for the simulations, respectively.

Table 1: Table of settings and details of WRF-ARW simulations.

Setting	Detail
Domains (H1, H2, and H3)	3 grids with 2 nests
Grid Spacing in Domains	(12 km, 4 km, 1.33 km)
USGS Topographic Grid Scales in Domains	CONTROL Run: (10 arcmin, 2 arcmin, 0.5 arcmin) SMOOTH Run: (10 arcmin, 10 arcmin, 10 arcmin)
Model Top Level and Δp	(50 hPa, 25 hPa)
Time Step in Domains	(90 s, 30 s, 10 s)
Initial and Boundary Conditions	12-km North American Mesoscale Model
Land Surface	Noah Land Surface (Yang et al. 2011)
Surface Layer	Monin-Obukhov (Monin and Obukhov 1954)
Shortwave Radiation	MM5 Shortwave
Longwave Radiation	Rapid Radiative Transfer
Cumulus Convective Scheme in Domains	CONTROL and SMOOTH Runs: (ON, ON, OFF)
Boundary Layer Scheme	Mellor-Yamada-Janjić (Mellor and Yamada 1982; Janjić 2002)
Microphysics Scheme	Purdue-Lin (Lin et al. 1983)

Numerical simulations of the WRF-ARW model (Version 3.0.1) were performed with a model spin-up time of 10–18 h in order to resolve the antecedent and post synoptic-scale environments of the SPCZ. This simulation was initialized at 0000 UTC 26 November 2005. The initial and lateral boundary conditions originated from the 6-hourly North American Mesoscale Model Analysis (Grid 218) 12-km grids (Rutledge et al. 2006). The model top was situated at 50 hPa with a pressure interval of $\Delta p = 25$ hPa. In the two simulations, the time step was $\Delta t = 90$ s for the parent grid with a parent time step ratio of (1, 3, 3) or (90 s, 30 s, 10 s) for the three domains. As Table 1 shows, several parameterizations were used to model physical processes in this study,

including the Purdue-Lin microphysics (Lin et al. 1983) and Mellor-Yamada-Janjić boundary layer (Mellor and Yamada 1982; Janjić 2002) schemes. There is wide acceptance among numerical modelers in using the cumulus convective scheme at grid scales ≥ 4 km (Kain et al. 2006; Skamarock et al. 2008). Hence, the scheme was activated in grid H1 (12 km). Moreover, the scheme was activated in grid H2 (4 km) and evidently robust enough in simulating the convection associated with the SPCZ. The cumulus parameterization was deactivated in grid H3 so the model could explicitly resolve cumulus clouds at finer grid scales of 1.33 km (Kain et al. 2006; Skamarock et al. 2008).



Figure 3: WRF-ARW model domains. The outer model grid domain (H1: green rectangle) encloses two nested grid domains (H2: blue rectangle) and (H3: red rectangle). Domain H3 covers eastern Idaho. [Click image to enlarge.](#)

b. Justification of sensitivity experiments

As described earlier, the difference between the CONTROL and SMOOTH runs is the topographic grid scale with all other physical parameterizations remaining constant. A comparison of these topographic grid scales reveals major differences. In the Central Mountains, there are four narrow ridgelines and three tributary valleys in the CONTROL run and two elongated plateaus with two broad valleys in the SMOOTH run. The CONTROL run (Fig. 4a) resolves the three tributary valleys (Fig. 1). The Birch Creek Valley contains a shallower eastern boundary and the Big Lost River Valley lacks a major western boundary in the SMOOTH run. The Little Lost River Valley is poorly defined in Fig. 4b. These topographic differences affect the low-level flow and development of the convergence bands in the Snake River Plain (Andretta 2011). Hence, by comparing these two topographic grid scales, it is possible to determine the influence of the terrain *exclusively* on the flow regimes (Fig. 2) forming the SPCZ. This explanation provides the justification for the following topographic sensitivity experiments.

5. Data processing

The WRF-ARW simulations were quality controlled by generating run-time reports of the model output variables. These log files were meticulously checked for run-time data errors and no problems were detected in the simulations. The model output was generated as netCDF files and then converted into Unidata General Meteorology Package (GEMPAK) (desJardins et al. 1991) format with the wrf2gem utility (Decker 2005). The data were stored in a file geodatabase and displayed in ESRI ArcGIS mapping software for publication. The figures presented in this manuscript are hourly snapshots or animations so discussions of the physical processes are limited by those temporal constraints.

The KSFY WSR-88D 3-h digital precipitation array product was created by summing the precipitation totals in each grid cell over a 3-h period. The weighted average of the snow and graupel accumulations was computed for the WRF-ARW simulations in GEMPAK (desJardins et al. 1991). This value equals the sum of the snow (QSNOW) and graupel (QGRAUPEL) mixing ratios at isobaric levels (750–500 hPa) and then calculated as a weighted average over that layer at each model grid point. The Fr was computed for the WRF-ARW simulations using GEMPAK and performed at two model grid points close to the airports at Spokane, WA (KSEG) and Boise, ID (KBOI) (Fig. 3). The weighted average wind speed equals the sum of the wind velocities at isobaric levels (850–650 hPa) and then calculated as a weighted average over that layer. The Brunt-Väisälä frequency was computed over the same depth. The effective height was estimated as the difference between the apex of the Central Mountains (3500 m) and the surrounding terrain (m). The potential vorticity was calculated for the WRF-ARW simulations in GEMPAK (desJardins et al. 1991) using equivalent potential temperature (θ_e) and the total wind in pressure coordinates for the model cross sections. The 9-point data smoothing algorithm in GEMPAK and ESRI ArcGIS mapping software was used in the final graphical presentations of several variables.

6. Results

This section is organized following the outline and recommendations in Schultz (2010). The main topics include discussions of past research, model validation, and the structure and environment of the SPCZ within the sensitivity experiments.

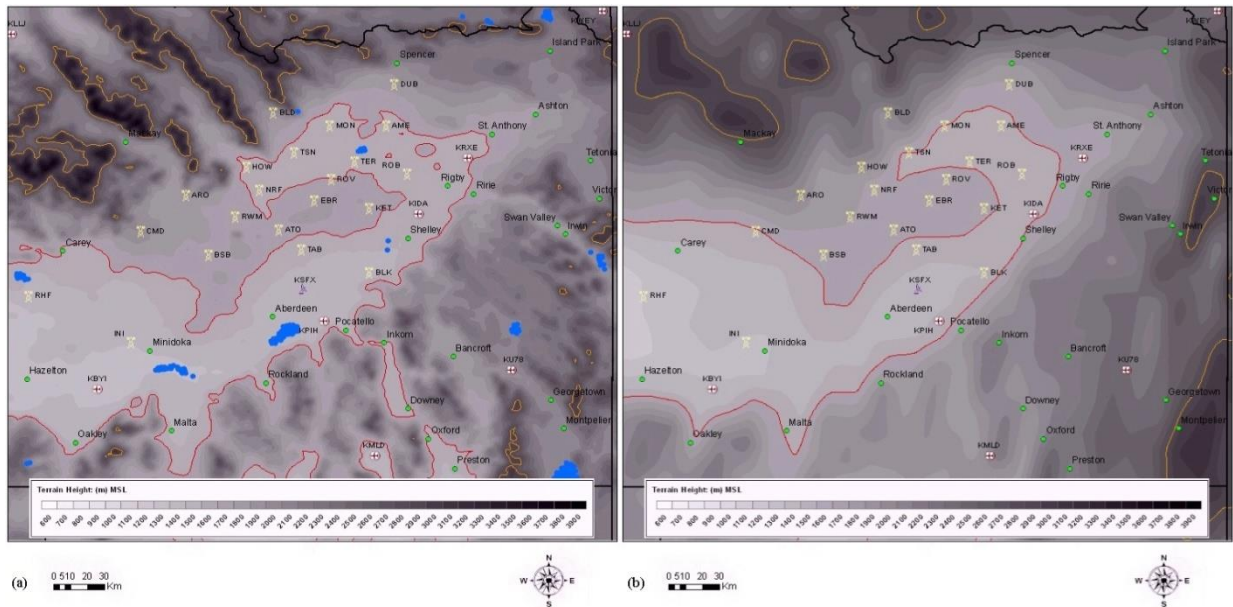


Figure 4: WRF-ARW model nested high-resolution grid H3 (1.33 km) with a) CONTROL (30-arcsec \approx 0.9-km) and b) SMOOTH (10-arcmin \approx 18-km) topography. The $z = 1500$ -m MSL (solid red contours) and $z = 2500$ -m MSL (solid orange contours) elevations indicate the key topographic features. The solid blue regions are bodies of water in the model. The various city and station identifiers use the same references illustrated in Fig. 1. *Click images to enlarge.*

a. Previous research

Andretta (2011) demonstrated model validation of the 26 November 2005 SPCZ event. The WRF-ARW model with a 4-km inner grid spacing predicted the horizontal convergence bands, vertical vorticity maxima and minima, and confluent radial velocity signatures in the surface and Doppler radar observations for this SPCZ episode. The 4-km WRF-ARW model also simulated the leeward (C1, C2, and C3) and windward (C4) convergence bands in the coarse 12-km surface observations.

b. Strengths and weaknesses of simulations

This section evaluates the strengths and weaknesses of the WRF-ARW numerical simulations. This model is validated through a comparison of the kinematic fields and precipitation totals for the KSFX WSR-88D observations and WRF-ARW runs (Grid H3). Andretta and Geerts (2010) discussed the Mesowest data and interpolation scheme mentioned in the following paragraph.

Figure 5 shows the model comparison with observations at 1800 and 2100 UTC for the horizontal divergence field. The Mesowest observations use a 12-km interpolated grid spacing for the wind vector and divergence fields. Due to the

possible large errors in the divergence field from poorly sampled station velocities, only the larger features are evaluated here. The major strength in the CONTROL run is the successful prediction of lee convergence bands C1, C2, and C3 in the upper plain. At 2100 UTC, the CONTROL run also simulates a small region of convergence between the KSFX WSR-88D location and Pocatello, ID (KPIH). However, band C4 in the Magic Valley is not as developed in the simulation versus the observations.

Figure 6 compares model with observations at 1800 and 2100 UTC for the vertical vorticity field. These vorticity structures contain alternating cyclonic and anticyclonic anomalies that develop from the low-level horizontal wind shear. The figure shows cyclonic (positive, P) and anticyclonic (negative, N) signs for the local vorticity. The CONTROL run agrees with the observations in generating a horizontal shear line with dipole (P1N1) in the Birch Creek Valley and cyclonic vorticity region P4 in the Magic Valley. The other dipoles in the model are much too fine for detection by the coarse 12-km Mesowest grid spacing. Nevertheless, one would expect a repetition of dipoles from similar shear lines along the other two tributary valleys in the model (Andretta 2011). Thus, the CONTROL run produces a series of three vorticity dipoles coinciding with the three tributary valleys.

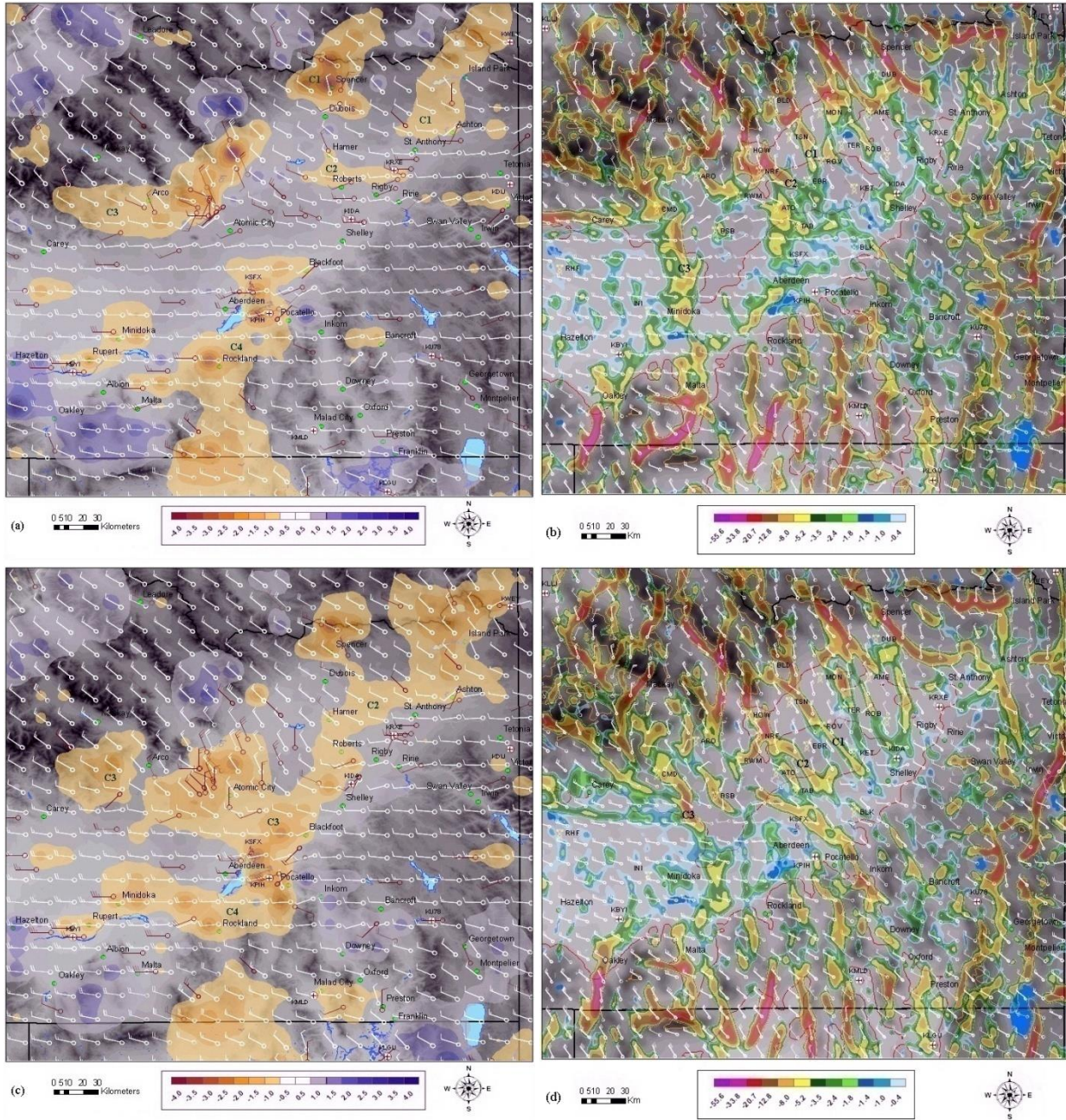


Figure 5: Surface wind barbs (brown and white, kt) and horizontal divergence (filled colors: 10^{-4} s^{-1}) for a) Mesowest at 1800 UTC, b) WRF-ARW Grid H3 run at 1800 UTC, c) Mesowest at 2100 UTC, and d) WRF-ARW Grid H3 run at 2100 UTC. The surface wind barbs (white, kt) are displayed at 12-km spacing in Mesowest. The 10-m AGL wind barbs (white, kt) are displayed at every third grid point in WRF-ARW output. Each full wind barb is 5 m s^{-1} (10 kt) and flag is 25 m s^{-1} (50 kt). *Click images to enlarge.*

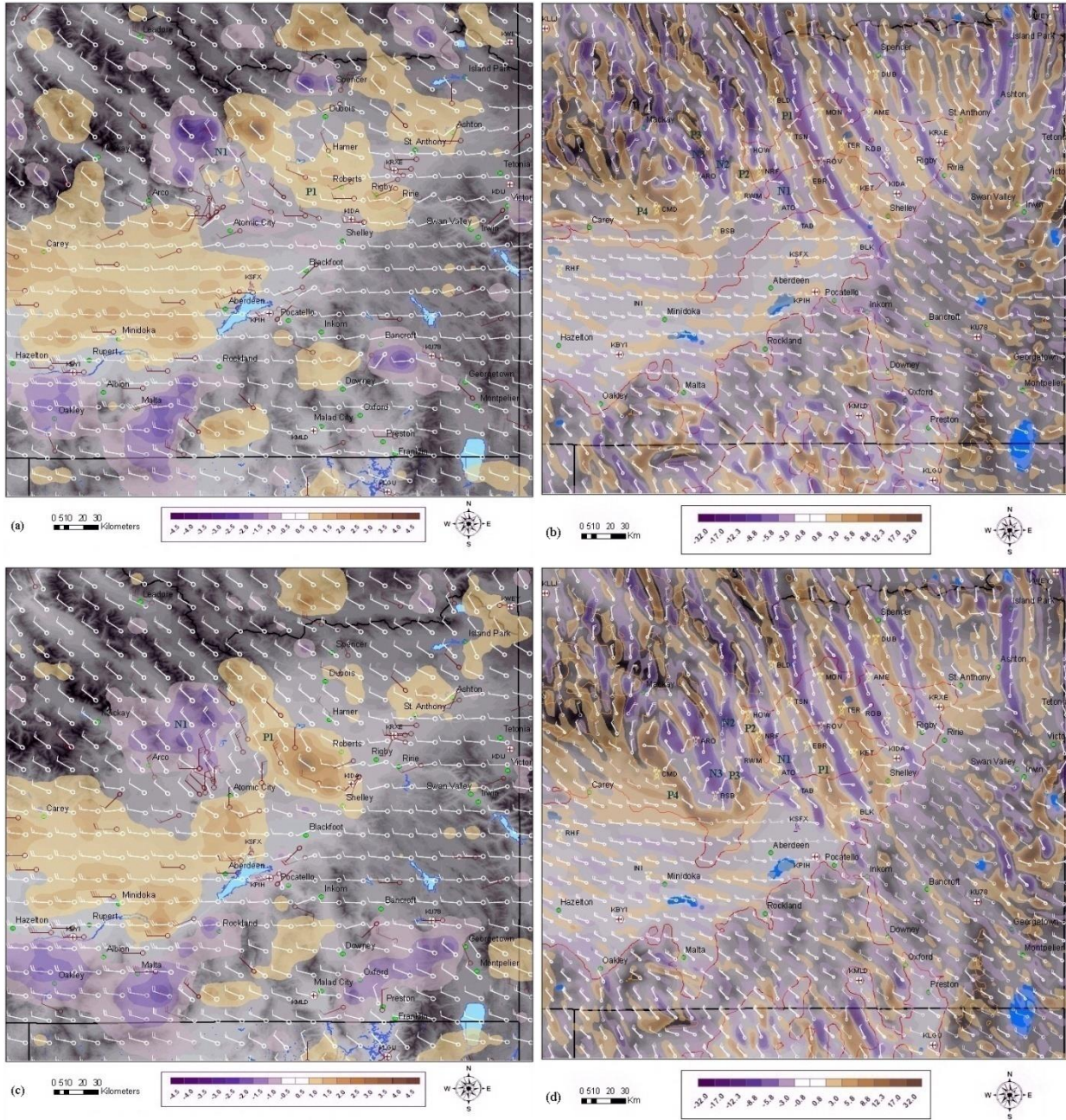


Figure 6: Surface wind barbs (brown and white, kt) and vertical vorticity (filled colors: 10^{-4} s^{-1}) for a) Mesowest at 1800 UTC, b) WRF-ARW Grid H3 run at 1800 UTC, c) Mesowest at 2100 UTC, and d) WRF-ARW Grid H3 run at 2100 UTC. Wind barb conventions as in Fig. 5. [Click images to enlarge.](#)

Given the previous pattern of the kinematic fields, this subsection explores the topographically generated precipitation patterns in the Snake River Plain. The presentation illustrates the 3-h precipitation accumulation that provides improved spatial and temporal continuity over the 1-h results during the SPCZ event. Accordingly, time lapses (26/1200–27/0000 UTC) of the 3-h precipitation

totals from the KSFx WSR-88D observations and the WRF-ARW model simulations are illustrated in Figs. 7 and 8, respectively. The KSFx WSR-88D used the equivalent reflectivity factor (Z) to rainfall (R) relationship of $Z = 300 R^{1.6}$ during this SPCZ event. The model forecasts the precipitation over the Snake Plain in the CONTROL and SMOOTH runs during the morning hours (1200–1500 UTC) associated with

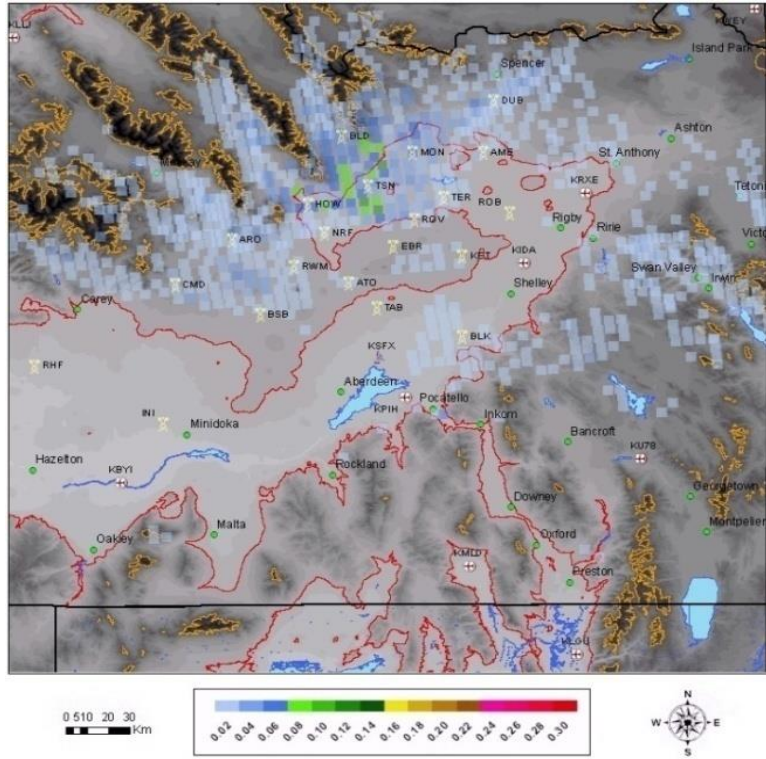


Figure 7: KSFX WSR-88D 3-h digital precipitation array (filled colors: in). *Click image to enlarge* for time lapse: 26/1200–27/0000 UTC.

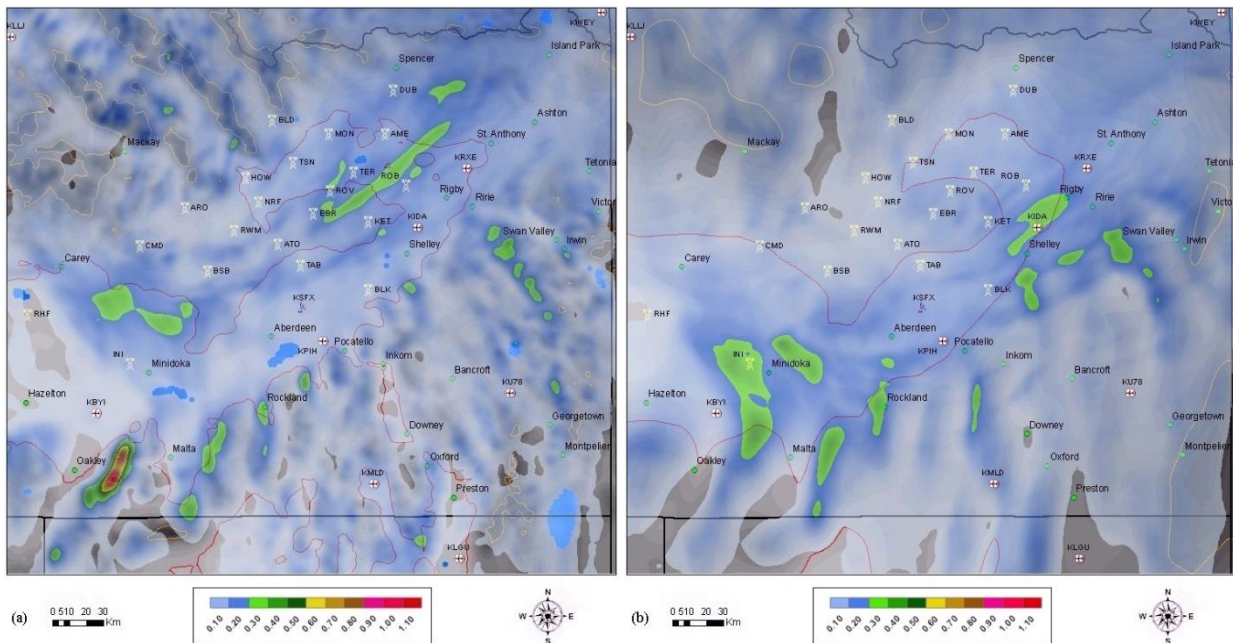


Figure 8: WRF-ARW Grid H3 3-h precipitation totals (filled colors: in) for a) CONTROL and b) SMOOTH runs. *Click images to enlarge* for time lapse: 26/1200–27/0000 UTC.

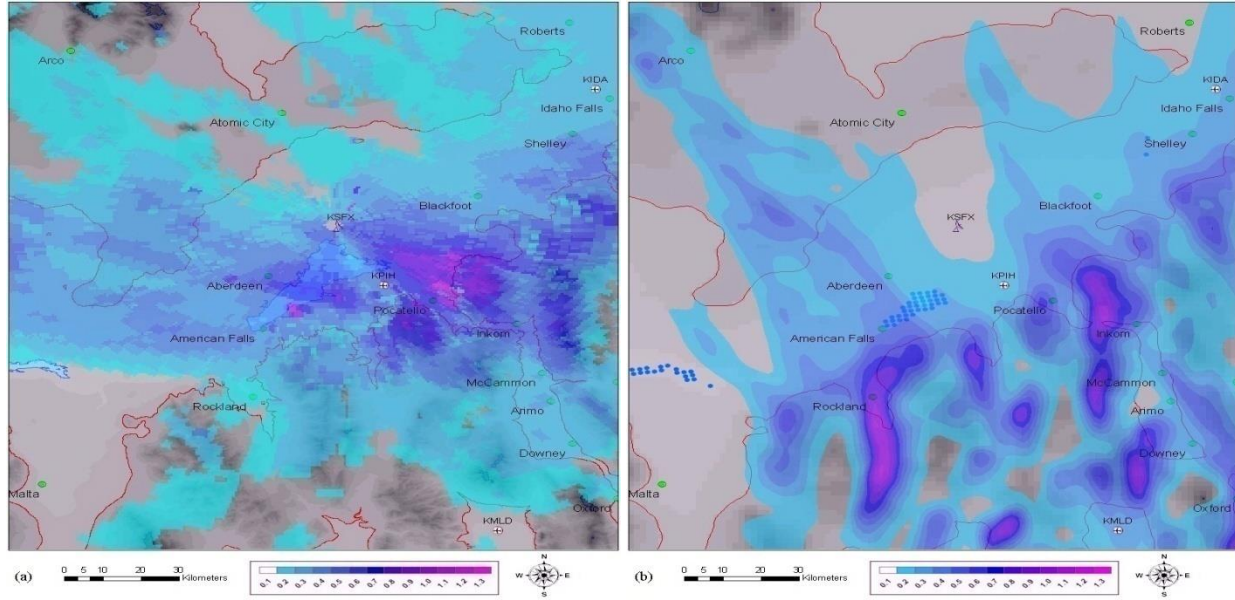


Figure 9: Snowmelt liquid water equivalent (SWE) 6-h (1800–0000 UTC) totals (filled colors: in) for a) KSFX WSR-88D and b) WRF-ARW Grid H3 CONTROL run. *Click images to enlarge.*

the passage of a Pacific cold front (Andretta and Geerts 2010; Andretta 2011). At 1800 UTC, the model runs reproduce the precipitation bands forming from topographic convergence aligned with long axes of the tributary valleys. Thus, these results are major strengths of the model simulations.

In the afternoon (~2100 UTC) hours, the model simulations indicate less precipitation over the Magic Valley versus the radar observations. Model simulations forecast heavier precipitation (0.51–0.76 cm (0.20–0.30 in)) near Pocatello, Inkom, and Rockland in the observations. However, both runs (Figs. 8a and 8b) display the western boundary of the precipitation shield near Minidoka (INI) or ≈ 50 km east of the radar observations near Richfield (RHF). Andretta (2011) found that sublimation (drying) and subsidence in the lower troposphere (850–700 hPa) of the Magic Valley contributes to this difference. Consequently, this result is a weakness of the numerical simulations.

The final comparison focuses on the total precipitation that fell with the SPCZ from 1800–0000 UTC. Figure 9 shows the derived snowmelt liquid water equivalent (SWE) using $Z = 75 S^2$ (Andretta and Geerts 2010), where Z is equivalent reflectivity factor and S is snowmelt liquid-water equivalent 6-h totals for the KSFX WSR-88D observations and WRF-ARW CONTROL run. In the

upper plain, the model SWE simulates the spatial distribution of two to three bands. In the lower plain from between Blackfoot and KPIH to Inkom, the model SWE is ≈ 70 –90% of the observations. As noted earlier, the model underpredicts the SWE in the Magic Valley.

c. Topographic flow blocking

To assess the degree of flow blocking by the mountains prior to SPCZ formation (Andretta 2011), the synoptic-scale flow is examined for the 12-km outer grid (H1) in the CONTROL and SMOOTH simulations. As noted earlier, the Fr describes the ratio of the kinetic to the potential energy for flow moving around or over an obstacle.

Figure 10 shows the 1200 UTC Fr calculated from GEMPAK for the outer domain (H1) in the CONTROL and SMOOTH runs. This time corresponded to several hours prior to SPCZ genesis.

As indicated in Eq. (1), the layer of the \bar{U} wind speed is the effective terrain depth (H) from 850–650 hPa. The approaching low to mid-level flow is oriented from the northwest to west direction or roughly normal to the Central Mountains and Southern Highlands. Andretta (2011) demonstrated that these topographic features (Fig. 1) block the low-level flow and divert it into the Snake River Plain.

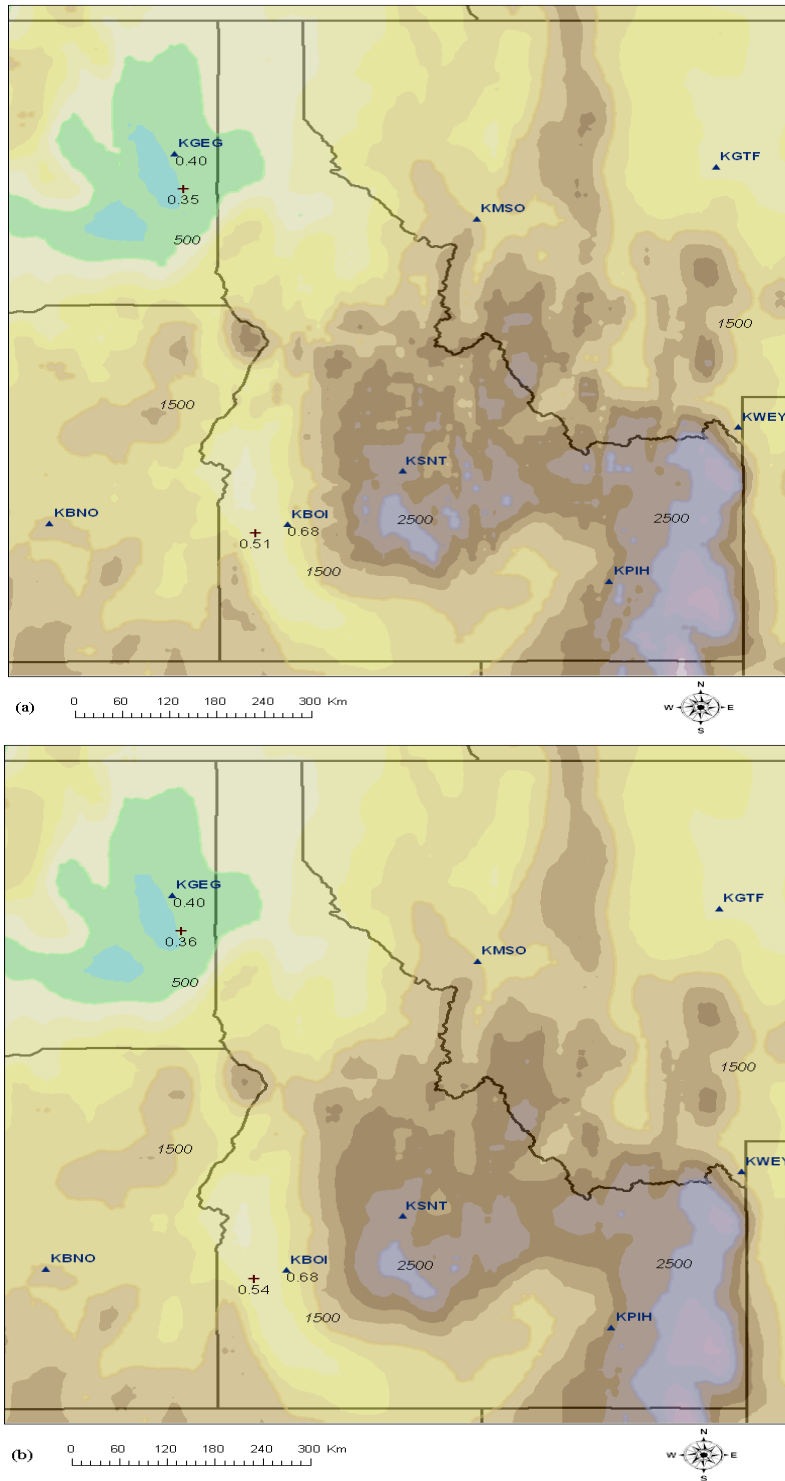


Figure 10: WRF-ARW Grid H1 for a) CONTROL and b) SMOOTH runs. The Fr (1200 UTC) are displayed at the airports (KEGG and KBOI) (dark blue triangles with black labels) based on upper-air soundings and computed in the model runs at nearby grid points (red crosses with black labels). The terrain contours at $z = 500, 1500,$ and 2500 m MSL (italic black labels) are indicated by solid thick green, brown, and purple lines, respectively. *Click images to enlarge.*

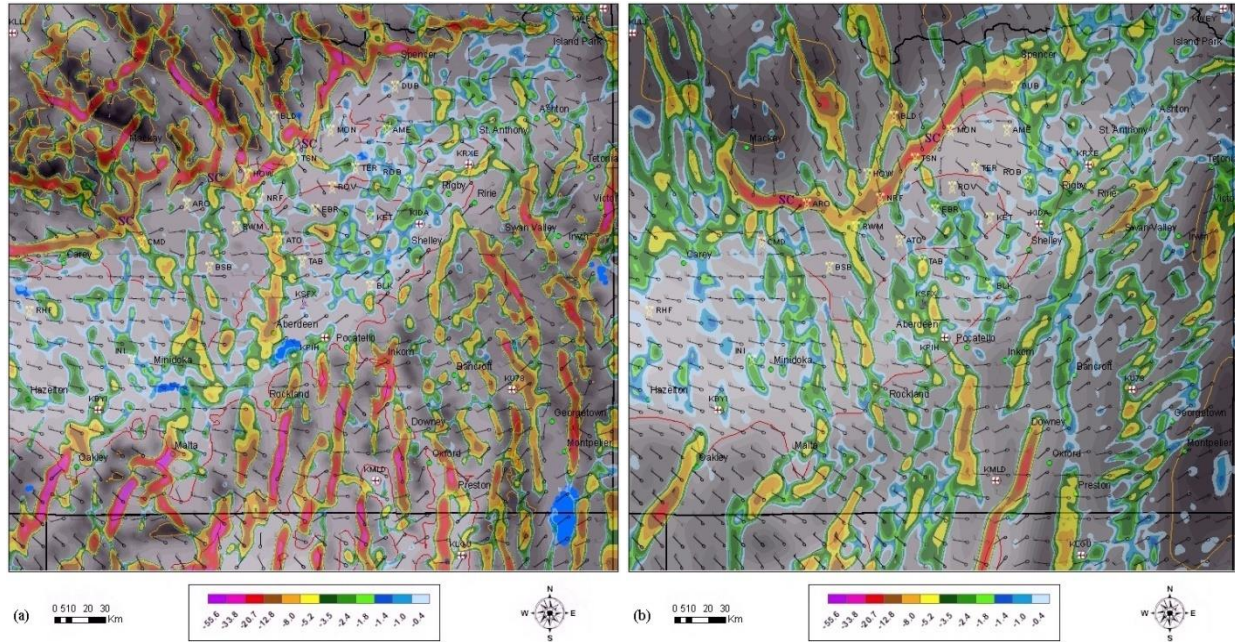


Figure 11: WRF-ARW Grid H3 10-m wind barbs (at every 8th grid point; black, kt) and horizontal divergence (filled colors, 10^{-4} s^{-1}) for a) CONTROL and b) SMOOTH runs. Each full wind barb is 5 m s^{-1} (10 kt) and flag is 25 m s^{-1} (50 kt). Annotations are described in the text. SC denotes a speed convergence band. *Click images to enlarge for time lapse: 26/1200–27/0000 UTC.*

Andretta (2011) calculated Fr of 0.40 and 0.68 at Spokane (KGEG) and Boise (KBOI) airports in the 1200 UTC soundings, respectively. These values are indicated in Figs 10a and 10b. Moreover, similar values are computed at the model grid points near these airports in both simulations. The positive values of the Fr from Eq. (1) in the figures indicate statically stable flow. In the CONTROL run (Fig. 10a), the flow blocking is more pronounced northwest of the Central Mountains ($0.0 < \text{Fr} < 0.5$) versus the southwest side of the barrier. However, in the SMOOTH run (Fig. 10b), the terrain blocking is reduced slightly (larger Fr) along the southwestern periphery of the Central Mountains and Southern Highlands. This shallower flow blocking by the Southern Highlands in the SMOOTH run may also explain the paucity of terrain-induced precipitation (1800–2100 UTC) in parts of the Magic Valley.

d. Kinematic structure of SPCZ

Andretta (2011) hypothesized that the SPCZ consisted of leeward and windward convergence components in stable blocked flow. It was previously demonstrated in section 6c that the model Fr was

small enough for stable flow blocking by the Central Mountains. This section addresses the research question: Does the CONTROL terrain grid scale produce finer convergence bands and vorticity structures? The horizontal structure of the SPCZ is examined in the kinematic wind velocity derivatives and reflectivity fields. A time lapse (26/1200–27/0000 UTC) of the surface wind and horizontal divergence is indicated in Fig. 11 for both runs of the WRF-ARW model. Between 1200–1500 UTC, the model simulations develop a speed convergence band influenced by flow deceleration from the valley exit regions to the broader plain. This feature persists over several hours. Figure 11 indicates three convergence bands (C1, C2, and C3) forming in the lee of the Central Mountains and aligned with the long axes of the tributary valleys. However, these leeward convergence bands are generally longer and stronger in the CONTROL run. Band C3 is the strongest band in the lower plain with several, linear, intersecting, zonal, convergent bands in the Magic Valley. These along-valley convergence bands are influenced by flow deceleration in the Magic Valley, forming the windward component of the SPCZ (Andretta 2011).

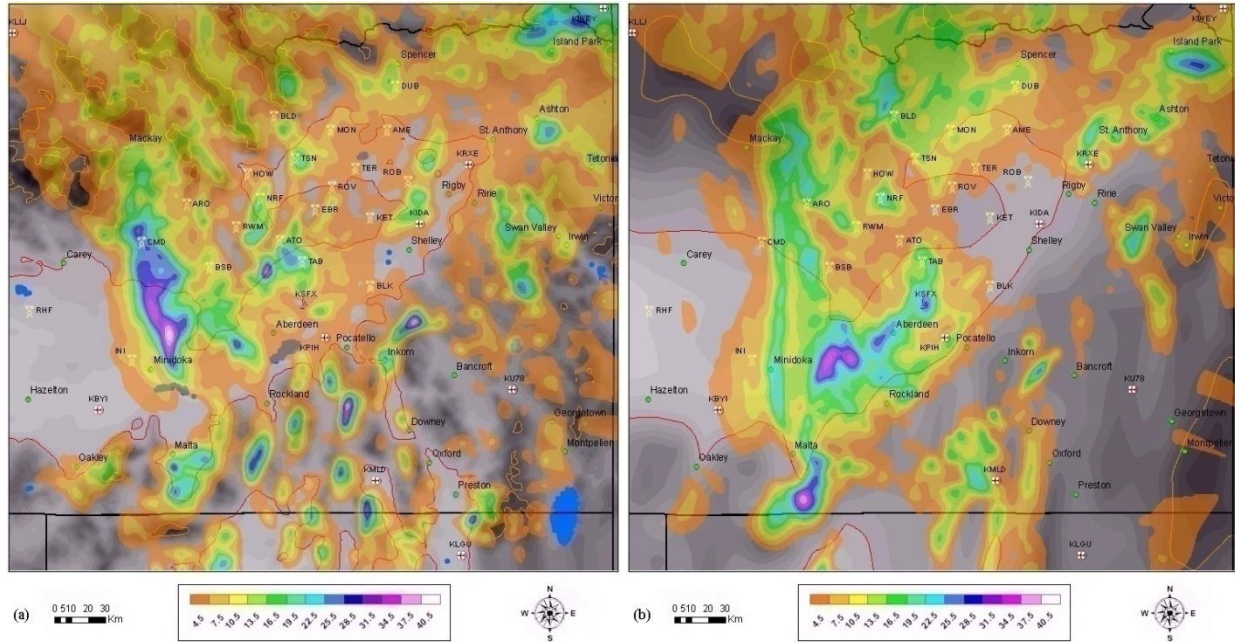


Figure 13: WRF-ARW Grid H3 750–500 hPa layer weighted average of (QSNOW + QGRAUPEL) mixing ratios (filled colors: $10^{-2} \text{ g kg}^{-1}$) for a) CONTROL and b) SMOOTH runs. The annotations are described in the text. *Click images to enlarge* for time lapse: 26/1200–27/0000 UTC.

1983) scheme is used in both simulations. The key difference between the runs is the poorly defined Little Lost River Valley and the presence of a weaker precipitation band (B2) in the SMOOTH run. During the local afternoon hours (1900–2300 UTC), the CONTROL run generates heavy snow and graupel totals in band B3 near Aberdeen, between Pocatello and Inkom, and near Rockland. This result agreed with the observations (Andretta and Geerts 2010). The intensity of band B3 in the CONTROL run was augmented by weak conditional instability in the form of surface-based (SB) CAPE $\approx 40\text{--}80 \text{ J kg}^{-1}$. As Fig. 14 shows, this CAPE was released during the afternoon hours (2100–2300 UTC). By contrast, the SMOOTH run only generates comparable snow and graupel accumulations in band B3 near Rockland. The smoother terrain clearly influences the generation of weaker SPCZ-related precipitation in the lower plain.

f. Vertical structure of SPCZ

This section investigates the influence of the terrain grid scales on the convergence patterns, related circulations, and convection. Figures 15 (1800 UTC) and 16 (2100 UTC) show two cross sections through the Snake River Plain and Magic Valley, constructed roughly perpendicular to the convergence bands and associated circulations. Figures 17 and 18 indicate the horizontal

convergence, circulation wind arrows, and reflectivity signatures over these regions.

The reflectivity signatures are labeled alphabetically with capital letters from west to east in Figs. 17 and 18. Colder air is located in the Magic Valley. The atmosphere is generally moist statically stable in both runs; the stability decreases in the vicinity of the topographic convergence with the spreading of the θ_e isentropes. The storms slightly tilt with height into the colder air aloft from the vertical wind shear and hydrometeor advection.

However, there are some differences between the simulations. In Fig. 17, for storms A, B, and C in the lee of the Central Mountains, the low-level convergence is deeper and stronger in the CONTROL run. By contrast, in Fig. 18, cores B and C appear as elevated signatures. The convergence field extends deeper into storm D and E in the CONTROL run. In Fig. 17, the reflectivity maxima differ over the higher terrain east of the Lower Snake River Plain. In the CONTROL run, storm B (10–25 dBZ) extends across the mountain range east of Inkom in moist stable upslope flow (windward convergence) (Whiteman 2000). This lifting mechanism was responsible for moderate to heavy snowfall recorded in the surface and radar observations (Andretta and Geerts 2010; Andretta 2011).

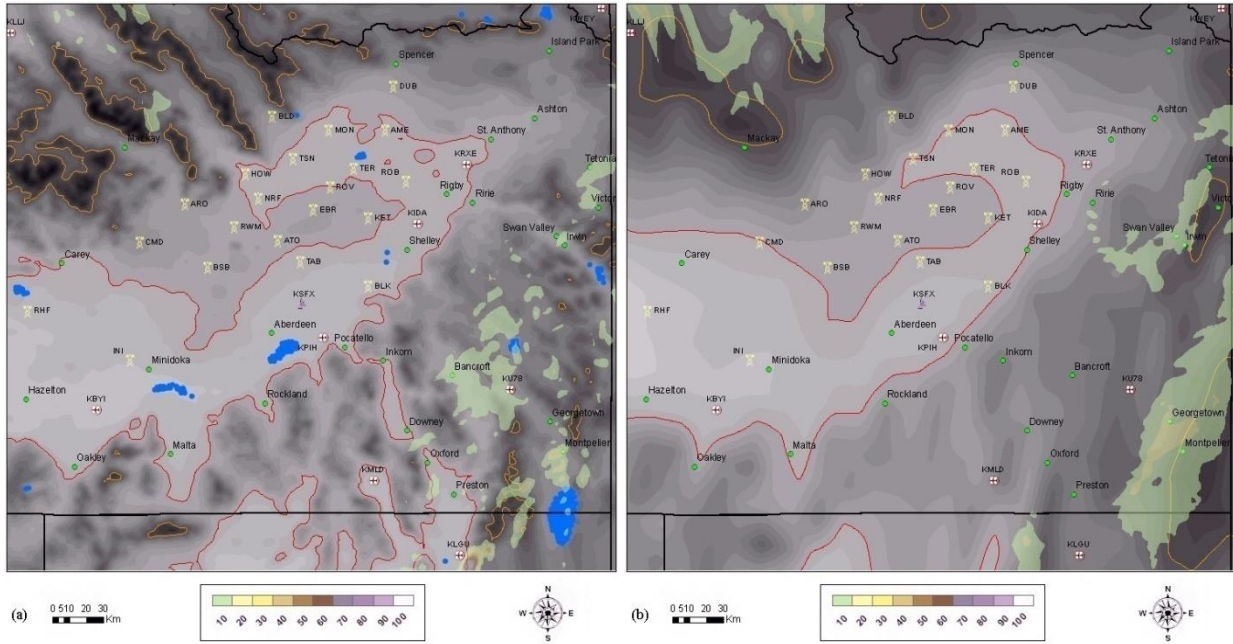


Figure 14: WRF-ARW Grid H3 SBCAPE (filled colors: $J\ kg^{-1}$) for a) CONTROL and b) SMOOTH runs. The annotations are described in the text. *Click images to enlarge* for time lapse: 26/1200–27/0000 UTC.

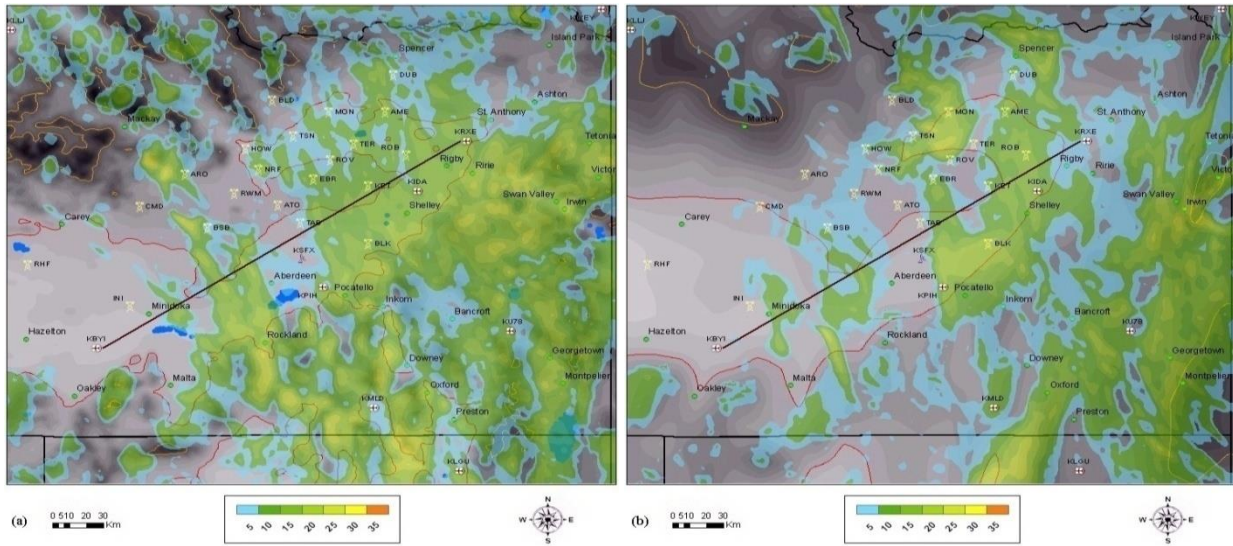


Figure 15: WRF-ARW Grid H3 composite reflectivity (filled colors: dBZ) at 1800 UTC for a) CONTROL and b) SMOOTH runs. The thick brown line indicates the cross section from Burley, ID (KBYI) to Rexburg, ID (KRXE). *Click images to enlarge*.

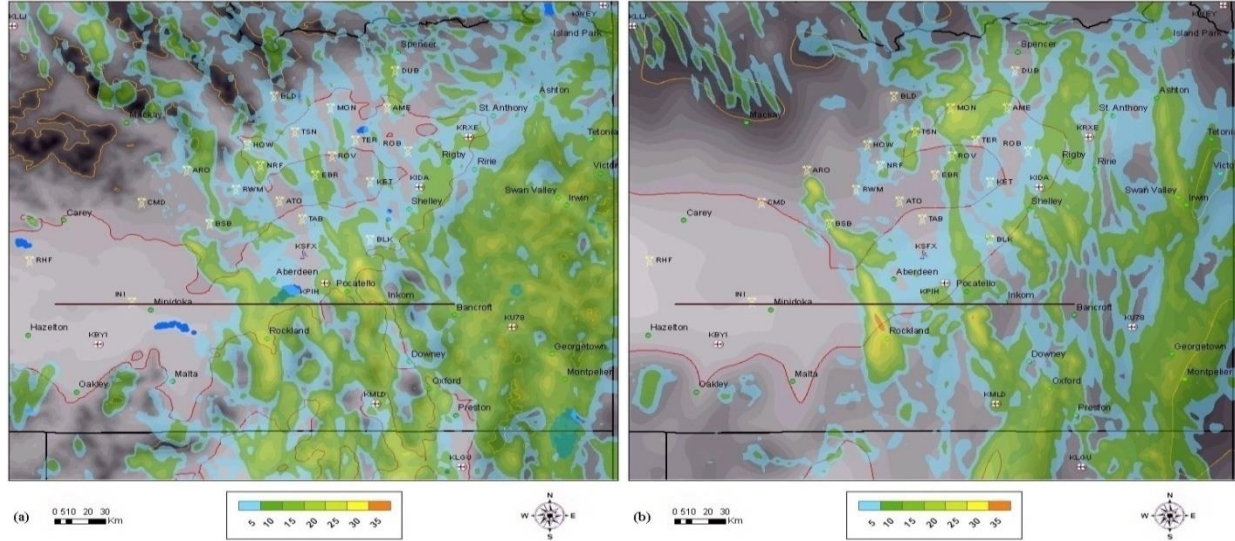


Figure 16: WRF-ARW Grid H3 composite reflectivity (filled colors: dBZ) at 2100 UTC for (a) CONTROL and (b) SMOOTH runs. The thick brown line indicates the cross section from latitude and longitude coordinates $(-114.00, 42.82)$ to $(-112.00, 42.82)$. *Click images to enlarge.*

g. Band stability in SPCZ

This subsection explores the band stability within the convective storms in both simulations and addresses the following question: Does the terrain modulate the vorticity anomalies within the reflectivity signatures of the SPCZ? Research has indicated that potential vorticity (PV) banners occur downwind of mountain passes and terrain gaps (Aebischer and Schär 1998; Schär et al. 2003). Accordingly, the following paragraphs examine the vorticity anomaly structures in both simulations associated with the terrain-induced horizontal wind shear lines within the Upper Snake River Plain.

Figure 19 shows a transect from KBYI to KRXE (same as in Fig. 15) oriented roughly normal to the simulated reflectivity bands, circulations, and stabilities. The plots show θ_e and equivalent potential vorticity ($EPV < 0$). The EPV is computed in pressure coordinates from McCann (1995):

$$EPV = g \left[\frac{\partial \theta_e}{\partial x} \frac{\partial v}{\partial P} - \frac{\partial \theta_e}{\partial y} \frac{\partial u}{\partial P} - \frac{\partial \theta_e}{\partial P} \left(\frac{\partial v}{\partial x} - \frac{\partial u}{\partial y} + f \right) \right] \quad (2)$$

where (u, v) is the actual horizontal wind; horizontal gradients of θ_e are computed on isobaric surfaces and $\zeta_z = \frac{\partial v}{\partial x} - \frac{\partial u}{\partial y}$ is the z-component of relative vorticity.

In Eq. (2), the first two terms are proportional to vertical shear of the horizontal wind and horizontal θ_e gradients; the last term is the product of the

convective and inertial stabilities. In a frictionless atmosphere, EPV is conserved under dry and moist adiabatic conditions. The atmosphere is unstable where $EPV < 0$ and occurs under convective instability ($\partial \theta_e / \partial P > 0$) or under horizontal (inertial) instability ($\zeta_z < -f$). First, the negative EPV ($\partial \theta_e / \partial P > 0$) is released through layer lifting in a saturated atmosphere (Rogers and Yau 1989; Schultz and Schumacher 1999; Kirshbaum and Durran 2005a,b). The atmosphere is unstable where the vertical component of relative vorticity is smaller than the planetary vorticity ($\zeta_z < -f$). This condition is satisfied near anticyclonic (negative) banners of vorticity. Negative EPV also occurs in the atmosphere under the presence of weak convective stability to upright convection and weak positive inertial (horizontal) forcing. This condition is called potential symmetric instability (PSI).

The presence of these instabilities does not guarantee that they were released during this SPCZ episode. Furthermore, the physical processes governing the formation of snowbands from these instabilities remain unclear (Schumacher et al. 2010; Andretta 2011). Since a moist environment is conducive for PV bands to organize, contours of relative humidity (solid light green contours: RH = 80%) are also depicted in the figures. Hence, the goal is to find regions of instability where $EPV < 0$ (solid purple contours) and deep moisture with RH $> 80\%$ (Seltzer et al. 1985).

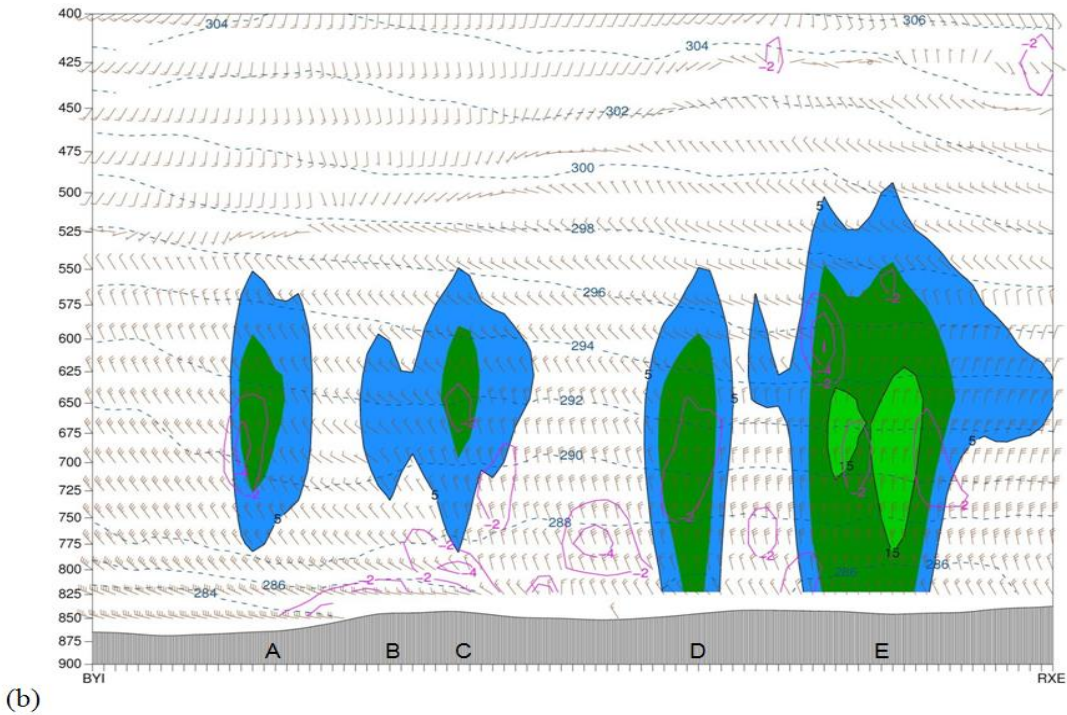
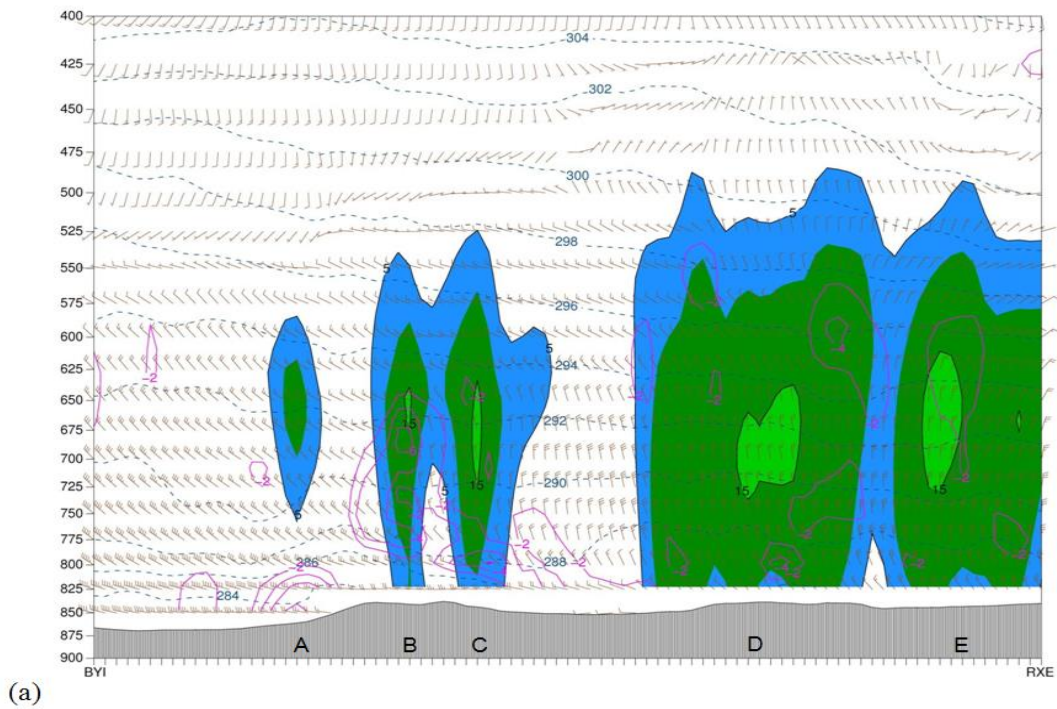


Figure 17: WRF-ARW Grid H3 cross sections from KBYI to KRXE at 1800 UTC (in Fig. 15) simulated reflectivity (filled colors with solid black contours and black labels: dBZ), horizontal divergence (solid pink contours and pink labels: 10^{-4} s^{-1}), wind barbs (brown: kt), and θ_e (dashed blue contours and blue labels, K) for a) CONTROL and b) SMOOTH runs. Ordinate values are pressure (hPa). Reflectivity cores are labeled (A, B, C, D, and E). *Click images to enlarge.*

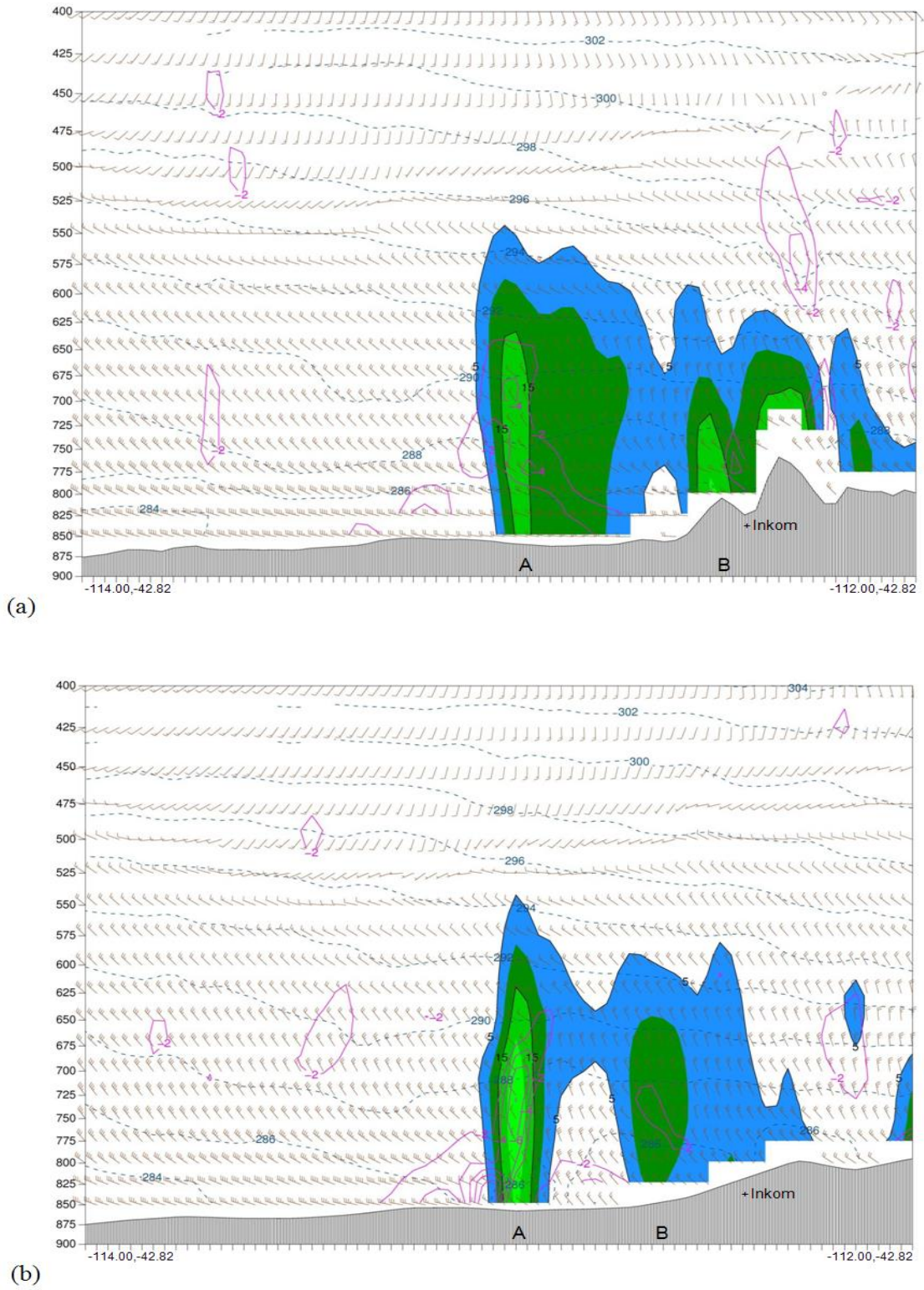


Figure 18: As in Fig. 17, but from (-114.00, 42.82) to (-112.00, 42.82) at 2100 UTC (in Fig. 16). Reflectivity cores are labeled (A and B) in the transect. [Click images to enlarge.](#)

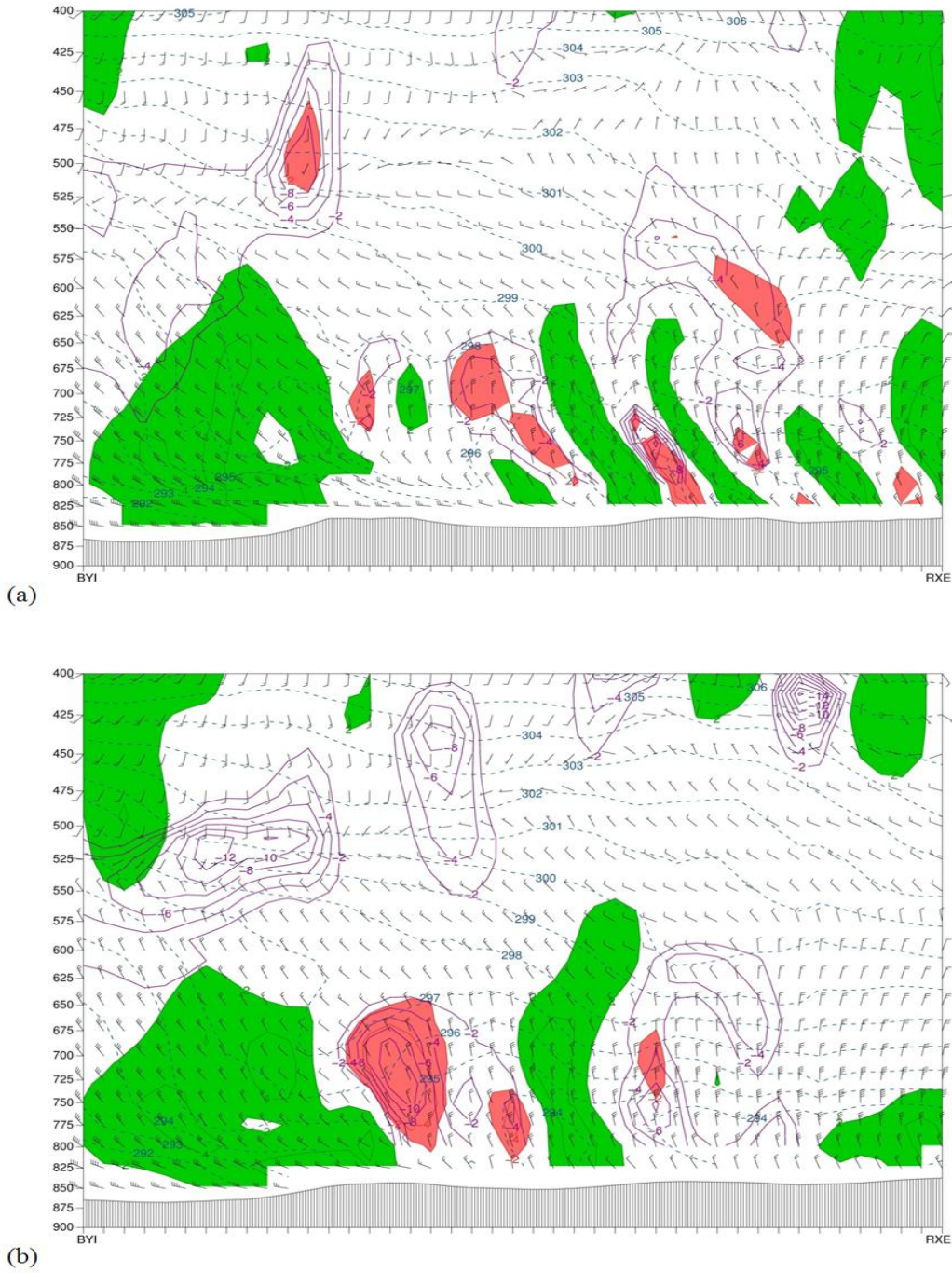


Figure 19: WRF-ARW Grid H3 from KBYI to KRXE simulated reflectivity (filled colors with solid black contours and black labels, dBZ), wind barbs (black, kt), absolute vorticity [filled green (positive) and filled red (negative) contours and labels: 10^{-4} s^{-1}], EPV (solid purple contours with purple labels for EPV < 0: $10^{-7} \text{ K kg}^{-1} \text{ m}^2 \text{ s}^{-1}$ or 10^{-1} PVU), θ_e (dashed blue contours and blue labels, K), circulation wind arrows (solid brown, $\text{m}^2 \text{ s}^{-2}$), and relative humidity (solid light green contours with light green labels for RH = 80%) for a) CONTROL and b) SMOOTH runs. Ordinate values are pressure (hPa). The annotations are described in the text. (Click images to enlarge for time lapse: 26/1800–26/2300 UTC).

A time lapse (26/1800–26/2300 UTC) of the EPV is provided in Fig. 19 for both runs of the WRF-ARW model. In the Magic Valley just northeast of KBYI, $EPV < 0$ is associated with the convective instability ($\partial\theta_e/\partial P > 0$) with θ_e folds at the lower levels from 850–725 hPa. This instability is associated with lifting of a stable layer, containing saturated surface air and unsaturated air aloft, along the gentle slope of the Magic Valley. In the Upper Snake River Plain, EPV became negative related to the horizontal instability ($\zeta_z < -f$) in the anticyclonic vorticity banners exiting the tributary valleys. In some instances, inertial instability has been associated with the organization and maintenance of convection along anticyclonic banners (Knox 2003; Schultz and Knox 2007).

Over a period of several hours (Fig. 19), the terrain-induced convergence carries the negative EPV aloft in the updrafts (solid circulation arrows). This EPV became tilted with height from the vertical wind shear. These circulations in the upright reflectivity signatures are slightly tilted into the colder air (850–400 hPa). The time lapses suggest that this horizontal instability is periodically lifted along the moist isentropes and released near these storms during the SPCZ event. This ascent is most pronounced near reflectivity signatures C and D in both cases. These numerical simulations indicate that the terrain-driven circulations and simulated reflectivity signatures are generally more defined and stronger in the CONTROL run.

7. Conclusions

The Snake River Plain Convergence Zone (SPCZ) is a topographic mesoscale weather system that occurs in the cold season. It consists of leeward and windward flow regimes under low Fr (stable blocked flow) in a post-cold-frontal environment. This study examined the dynamics of a fall 2005 SPCZ event with the WRF-ARW model using two topographic grid scales.

In particular, the CONTROL run of the model reproduced the leeward and windward convergent components of the zone, relative vertical vorticity maxima and minima, and snowbands. In general, these features were stronger and more persistent in the CONTROL run. By comparison, the SMOOTH run did not simulate the middle vorticity dipole in the Little Lost River Valley. The SMOOTH run also missed the stable upslope flow in the Pocatello-Inkom area. By comparison, the CONTROL run reproduced locally strong convergence and heavy snow bands in the observations within the Pocatello-

Inkom region. In both runs, the model precipitation field did not extend as far west as the observations in the Magic Valley. Despite this limitation, both simulations provided insights into the vertical structure of the zone. The SPCZ contained upright reflectivity signatures with circulations that slightly tilted with height into the colder air aloft from the vertical wind shear and hydrometeor advection.

The topographic convergence was the primary lifting mechanism for the snowbands in the simulations. These bands were enhanced in the presence of conditional and convective instabilities. During the afternoon hours of the event, weak conditional instability occurred along an intense snowband in the Arco Desert and Lower Snake River Plain. Convective instability occurred in a lighter area of snow as a layer of moist stable air was lifted along the gentle elevation rise of the Magic Valley and lower plain. Inertial instability, that formed within the anticyclonic (negative) vorticity minima in the Upper Snake River Plain, may have enhanced some snowbands. The terrain-driven circulations and simulated reflectivity signatures were generally more defined and stronger in the CONTROL run.

In retrospect, this sensitivity study should help the operational weather forecasting community understand the physical processes and environment that occur during SPCZ episodes.

ACKNOWLEDGMENTS

The author would like to thank several reviewers for feedback on this paper.

REFERENCES

- Aebischer, U., and C. Schär, 1998: Low-level potential vorticity and cyclogenesis to the lee of the Alps. *J. Atmos. Sci.*, **55**, 186–207.
- Andretta, T. A., 2002: Climatology of the Snake River Plain convergence zone. *Natl. Wea. Dig.*, **26**(4), 37–51.
- , 2011: Forcing, properties, structure, and antecedent synoptic climatology of the Snake River Plain convergence zone of eastern Idaho: Analyses of observations and numerical simulations. Ph.D. dissertation, University of Wyoming, 234 pp.
- , and D. S. Hazen, 1998: Doppler radar analysis of a Snake River Plain convergence event. *Wea. Forecasting*, **13**, 482–491.

- , and B. Geerts, 2010: Heavy snowfall produced by topographically induced winds in the Snake River Plain of eastern Idaho: Part I: Observational analysis. *Electronic J. Severe Storms Meteor.*, **5**, 1–33.
- Crook, N. A., T. L. Clark, and M. W. Moncrieff, 1991: The Denver cyclone. Part II: Interaction with the convective boundary layer. *J. Atmos. Sci.*, **48**, 2109–2126.
- Decker, S. G., 2005: wrf2gem: A program to convert WRF netCDF output to GEMPAK format. Preprints, *6th WRF/15th MM5 Users' Workshop*, Boulder, CO, NCAR, 3.44.
- desJardins, M. L., K. F. Brill, and S. S. Schotz, 1991: Use of GEMPAK on Unix workstations. Preprints, *Seventh International Conf. on Interactive Information and Processing Systems for Meteorology, Oceanography, and Hydrology*, New Orleans, LA, *Amer. Meteor. Soc.*, 449–453.
- Grasso, L. D., 2000: The differentiation between grid spacing and resolution and their application to numerical modeling. *Bull. Amer. Meteor. Soc.*, **81**, 579–580.
- Haltiner, G. J., and F. L. Martin, 1957: *Dynamical and Physical Meteorology*. McGraw-Hill, 470 pp.
- Holton, J. R., 2004: *An Introduction to Dynamic Meteorology*. Academic Press, 535 pp.
- Janjić, Z. I., 2002: Nonsingular implementation of the Mellor-Yamada Level 2.5 scheme in the NCEP Meso model. NCEP Office Note No. 437, 61 pp. [Available online at <http://www.emc.ncep.noaa.gov/officenotes/newer/notes/on437.pdf>.]
- Kain, J. S., S. J. Weiss, J. J. Levit, M. E. Baldwin, and D. R. Bright, 2006: Examination of convection-allowing configurations of the WRF model for the prediction of severe convective weather: The SPC/NSSL Spring Program 2004. *Wea. Forecasting*, **21**, 167–181.
- Kirshbaum, D. J., and D. R. Durran, 2005a: Atmospheric factors governing banded orographic convection. *J. Atmos. Sci.*, **62**, 3758–3774.
- , and —, 2005b: Observations and modeling of banded orographic convection. *J. Atmos. Sci.*, **62**, 1463–1479.
- Knox, J. A., 2003: Inertial instability. *Encyclopedia of the Atmospheric Sciences*, J. Holton, J. Pyle, and J. Curry, Eds., Academic Press, 1004–1013.
- Lin, Y.-L., R. D. Farley, and H. D. Orville, 1983: Bulk parameterization of the snow field in a cloud model. *J. Climate Appl. Meteor.*, **22**, 1065–1092.
- Mass, C. F., and G. K. Ferber, 1990: Surface pressure perturbations produced by an isolated mesoscale topographic barrier. Part I: General characteristics and dynamics. *Mon. Wea. Rev.*, **118**, 2579–2596.
- McCann, D. W., 1995: Three-dimensional computations of equivalent potential vorticity. *Wea. Forecasting*, **10**, 798–802.
- Mellor, G. L., and T. Yamada, 1982: Development of a turbulence closure model for geophysical fluid problems. *Revs. Geophys. Space Phys.*, **20**, 851–875.
- Monin, A. S., and A. M. Obukhov, 1954: Basic laws of turbulent mixing in the surface layer of the atmosphere. *Tr. Akad. Nauk SSSR Geofiz. Inst.*, **24**, 163–187.
- Parish, T. R., 1982: Barrier winds along the Sierra Nevada mountains. *J. Appl. Meteor.*, **21**, 925–930.
- Reinecke, P. A., and D. R. Durran, 2008: Estimating topographic blocking using a Froude number when the static stability is nonuniform. *J. Atmos. Sci.*, **65**, 1035–1048.
- Rogers, R. R., and M. K. Yau, 1989: *A Short Course in Cloud Physics*. Academic Press, 290 pp.
- Rutledge, G. K., J. Alpert, and W. Ebuisaki, 2006: NOMADS: A climate and weather model archive at the National Oceanic and Atmospheric Administration. *Bull. Amer. Meteor. Soc.*, **87**, 327–341.
- Schär, C., M. Sprenger, D. Lüthi, Q. Jiang, R. B. Smith, and R. Benoit, 2003: Structure and dynamics of an Alpine potential vorticity banner. *Quart. J. Roy. Meteor. Soc.*, **129**, 825–855.
- Schultz, D. M., 2010: How to research and write effective case studies in meteorology. *Electronic J. Severe Storms Meteor.*, **5**, 1–18.
- , and P. N. Schumacher, 1999: The use and misuse of conditional symmetric instability. *Mon. Wea. Rev.*, **127**, 2709–2732; Corrigendum, **128**, 1573.
- , and J. A. Knox, 2007: Banded convection caused by frontogenesis in a conditionally, symmetrically, and inertially unstable environment. *Mon. Wea. Rev.*, **135**, 2095–2110.

- Schumacher, R. S., D. M. Schultz, and J. A. Knox, 2010: Convective snowbands downstream of the Rocky Mountains in an environment with conditional, dry symmetric, and inertial instabilities. *Mon. Wea. Rev.*, **138**, 4416–4438.
- Seltzer, M. A., R. E. Passarelli, and K. A. Emanuel, 1985: The possible role of symmetric instability in the formation of precipitation bands. *J. Atmos. Sci.*, **42**, 2207–2219.
- Skamarock, W. C., J. B. Klemp, J. Dudhia, D. O. Gill, D. M. Barker, M. Duda, X.-Y. Huang, W. Wang and J. G. Powers, 2008: A description of the Advanced Research WRF Version 3. NCAR Technical Note TN-475+STR, 113 pp. [Available online at http://www.mmm.ucar.edu/wrf/users/docs/arw_v3.pdf.]
- Whiteman, C. D., 2000: *Mountain Meteorology Fundamentals and Applications*. Oxford University Press, 355 pp.
- Yang, Z.-L., G.-Y. Niu, K. E. Mitchell, F. Chen, M. B. Ek, M. Barlage, L. Longuevergne, K. Manning, D. Niyogi, M. Tewari, and Y. Xia, 2011: The community Noah land surface model with multiparameterization options (Noah-MP): 2. Evaluation over global river basins. *J. Geophys. Res.*, **116**, D12110.

REVIEWER COMMENTS

[Authors' responses in *blue italics*.]

REVIEWER A (W. J. Steenburgh):***Initial Review:***

Recommendation: Accept with major revisions.

General comments: This paper uses numerical simulations to explore a fascinating and complex case of heavy snowfall in and around the Snake River Plain of southern Idaho. Intrigued, I spent a great deal of time examining Part I (Andretta and Geerts 2010) and radar data from the event, which I obtained from NCDC. The paper appears to provide insight into the processes responsible for the development of wind-parallel snowbands downstream of the Idaho Central Mountains, which represent one important component of the observed event, but the model fails to capture the blocking upwind of the Southern Highlands and the crescent-shaped band that extends over the Magic Valley (i.e., B4 and B5, Fig. 10, Andretta and Geerts 2010). In addition, insights into the processes responsible for the development of the wind-parallel bands are obscured by the hard-to-follow description in section 3f. This paper may be acceptable for publication if it presents a forthright analysis of the strengths and weaknesses of the control (CTL) simulation and a clearer analysis of the processes contributing to the development of the PV banners and precipitation bands. There is also a pressing need to define the SPCZ. In some respects, the title of the paper is misleading as the most insightful aspects of the paper concern the evolution and dynamics of the wind-parallel bands that form downstream of the Idaho Central Mountains.

The reviewer has made several good points that have been addressed in the amended manuscript. The strengths and weaknesses of the model simulations have required a separate section in the paper. The overall narrative of the SPZ event in terms of the various sections has been integrated better in this new version of the manuscript. The SPCZ lifecycle is described in terms of the kinematic variables, snowbands, stability, and EPV fields. A definition of the SPCZ based on the flow regimes and physical forces is also provided in the amended text. The title has remained unchanged because the paper focuses on simulations initialized with the same physical parameterizations but different terrain silhouettes. Hence, the analyses are based on the sensitivity of the selected terrain files for the CONTROL and SMOOTH simulations. Thank you for the review and your constructive points.

Major Revisions:

1. The abstract states that “A control simulation accurately reproduces the planetary boundary layer flow, convergence bands, vorticity belts, and snowbands in the zone”. Later in the paper it is argued that, “The model storm total precipitation also agreed favorably with surface and radar observations. Furthermore, the model simulated the hourly precipitation rates estimated by Doppler radar for a 1.33-km grid and these precipitation fields spatially corresponded with several convergence bands.” However, no careful analysis of the model fidelity is done in the paper. Instead, the reader is referred to Andretta (2011), a doctoral dissertation at the University of Wyoming. A more careful diagnosis of CTL should be presented in this EJSSM article, including a direct comparison of the radar-derived precipitation total (e.g., Fig. 2b, Andretta and Geerts) with that produced by the WRF for the same period. In addition, the following characteristics of CTL should be discussed and considered:

In order to address these issues, the model validation section has been expanded in the amended manuscript. I have added two new figures which compare the KSFY WSR-88D observations and CONTROL run (H3) using the kinematic fields: horizontal divergence and vertical vorticity. A storm total map masks the multi-hourly precipitation trends seen in the various stages of the SPCZ in two model runs and the observations. The three-hour

precipitation plots sufficiently capture those trends, address the model validation, and provide improved temporal resolution over traditional one-hour plots. In addition, I have added a second figure which compares the SPCZ-forced SWE (1800–0000 UTC: six-hour total) from the KSFX WSR-88D and CONTROL run. This effort should address all of your concerns.

The inability of CTL to capture low-level flow blocking produced by the Southern Highlands: For example, compare the CTL and the observed winds (from Andretta and Geerts 2010) at 2100 UTC. The observed winds along the base of the Southern Highlands near PIH are primarily along-barrier, whereas the modeled winds have a modest cross-barrier component. For example, at KPIH, the observed winds are WSW, whereas the WRF winds are W. As one moves further up plain, the observed along-barrier flow penetrates all the way to Idaho Falls, whereas the WRF winds in this area are W or NW.

The flow can approach a hypothetical barrier from one, many, or all directions. The Froude Number is the ratio of the kinetic energy (flow speed) versus the potential energy (barrier height). The low-level flow is contained in the Snake Plain between the Central Mountains and Southern Highlands. As discussed in Andretta (2011), this flow is diverted around the Central Mountains ($0.0 < Fr < 1.0$) prior to the SPCZ formation. There are also blocking effects by the Southern Highlands ($0.0 < Fr < 1.0$) in stable upslope flow. This point was demonstrated by Andretta (2011) in several SPCZ cases based on the regional soundings at KBOI and KGEG. I have expanded on these points in the amended manuscript. The WRF-ARW model simulates the topographic flow blocking by the Central Mountains and Southern Highlands as evidenced in the gridded analyses of the Froude Number for both the CONTROL and SMOOTH runs.

The inability of CTL to capture the crescent-shaped band over the Magic Valley: This is potentially a major weakness as that band is a contributor to the heavy snowfall observed during this event. It is only briefly mentioned in p. 6 and needs to be discussed in greater depth.

The comparison between the KSFX WSR-88D precipitation observations (DPA) and CONTROL run (H3) data sets is not exactly equivalent for several reasons. The radar observations are based on a specific Z-R relationship; the model is based on hydrometeor concentration and size. The model contains finer spatial coverage than the radar data. The CONTROL run produces precipitation in the eastern Magic Valley (INI: Minidoka) just not as far west (RHF: Richfield) as the radar observations. This weakness has been cited in the amended text of the manuscript. Moreover, the point of including the microphysics species [750–500 hPa layer average ($Q_{SNOW} + Q_{GRAUPEL}$)] is to show that the model generates snow and graupel in the Magic Valley but it does not all fallout as precipitation because of sublimation (drying) and subsidence occurring there. This was demonstrated in Andretta (2011) and has been cited in the amended manuscript. Surface precipitation is just one variable in the comparison and is not entirely representative of other diagnostics; the model does predict the timing and location of the low-level convergence bands and vorticity belts in the coarser 12-km interpolated Mesowest observations.

The inability of CTL to capture the spatial structure of the radar estimated storm-total SWE presented in Fig. 2b of Andretta and Geerts (2010) who note, “Snowfall exceeding 2.5 cm of SWE occurred in a southwest to northeast oriented band in the central lower plain from between Aberdeen and Blackfoot to the American Falls Reservoir. A second, parallel stripe of >1 in of SWE occurred closer to the Southern Highlands.” I simply don’t see this feature in the 3-h precipitation totals presented. Instead, the simulation appears to be dominated by wind-parallel precipitation bands. This needs to be more strongly emphasized.

Please see the above comments. I agree with your proposed solution and the need for a discussion of the strengths and weaknesses of the model runs. This information has been added to the revised manuscript (Section 6).

Items a–c above suggest that blocking and related precipitation enhancement upstream of the Southern Highlands is underdone. This is an important weakness of the model simulation that needs to be discussed in greater depth and reflected in the abstract.

The flow is blocked and diverted around the Central Mountains (lee convergence) and blocked by the Southern Highlands (windward convergence). I demonstrated this hypothesis with several other SPCZ cases in Andretta (2011). Sublimation effects and local subsidence explain the lack of a more westward boundary in the model QPF. Section 6 has been reorganized entirely.

Radar loops from the event clearly show the formation of wind-parallel bands downstream of the Idaho Central Mountains. This seems to be the primary strength of CTL, which produces similar bands, although it should be noted that there are some differences in coverage and intensity depending on the time examined. I don't think this is a major problem, but it should be noted.

This point has been underscored and discussed in the amended text of the manuscript (Section 6).

2. To facilitate comparison of between CTL/SMOOTH and the observations, the color fill scales in Figs. 4 and 5 should be identical. It appears that the WRF produces quite a bit more precipitation than the radar estimate. It is possible the radar estimate is underdone. If so, this should be noted. If the model is too wet, this should be noted.

There was no success in editing the shape file and extending the precipitation range for the KSFY WSR-88D DPA. Regarding the model QPF issues, the color legends are the same for the respective time steps. In particular, the color legends have the same scale and color palette from 1200 (FROPA) to \approx 1800 UTC. Since less precipitation occurs after 1800 UTC, the scales and legends were adjusted to reflect the lower precipitation maxima over eastern Idaho. Hence, the color legends are temporally consistent in the paper. Please see my earlier points on the comparison between the radar/surface and model estimates. I have highlighted the differences between the two data sets in the amended text of the manuscript.

3. Given the complexity of this case, the definition and role of the Snake River Plain Convergence Zone is ambiguous and needs to be more rigorously defined. In Andretta and Geerts (2010), Fig. 3d suggests that the convergence zone is oriented normal to the axis of the Snake River Plain. However, in this case there seem to be at least three major players, none of which seem to have a structure similar to that in Andretta and Geerts (2010, Fig. 3d). One is an along plain convergence zone that forms between NW flow emerging from the Idaho Central Mountains and flow along the Southern Highlands. The second is found flow coming up the Snake River Plain meets the northwesterly flow emerging from the Idaho Central Mountains near Arco and Atomic City. Both of these can be seen in MesoWest analyses presented in Andretta and Geerts (2010). The third includes the more localized convergence zones related to ridge-valley corrugations in the Idaho Central Mountains. Do I have this right? Can the author define Snake River Plain Convergence Zone and place this complex flow in its proper context?

This SPCZ event is similar to other cases (Andretta and Hazen 1998). In my defense, Fig. 3d was a simple cartoon of the "incipient" leeward convergence band (aligned with the Birch Creek tributary valley)—in the formation stage of the SPCZ. This figure was never intended to summarize the entire SPCZ lifecycle. I have provided definitions of the SPCZ in the amended manuscript. I have added a figure from the dissertation to support these points. The general flow pattern for an SPCZ event is N/NE post-frontal in the upper plain intersecting pressure-driven NW tributary valley flow, and intersecting W/SW post-frontal upvalley flow in the lower plain. Within these three wind currents, the SPCZ consists of several well-defined structures: leeward (upper plain: horizontally shear-induced convergence bands) and windward (lower plain: stable upslope convergence band) components. The reviewer can examine these flow regimes and related convergence bands in the new figure.

4. Sections 3d and 3e seem to add little to the paper. There's nothing in section 3d that builds upon the earlier section and 3e is also detached. It would make sense to integrate the stability discussion into section 3f.

The Results (Section 6) has been reorganized in the new paper to reflect your concerns.

5. The methodology for calculating the diabatic and frictional terms in Eq. (3) needs to be described.

The section on the PV budget equation has been removed from the paper.

6. I found section 3f, which is perhaps the most important section of the paper, to be quite confusing and difficult to follow. A coherent picture of the processes that produce the vorticity streamers and the wind-parallel snowbands simply never emerged. In addition, a PV budget equation is presented (Eq. 3) and an analysis presented in Fig. 15, but that figure is never really described. Instead, the convergence pattern in Fig. 7 is described. Predominantly cross-flow cross sections are presented, but the advection of PV in the cross flow direction is important. Although comparison of CTL and SMOOTH suggests that corrugations (i.e., valley-ridge) in the topography are important for generating the PV banners, a clear and coherent description of their generation, advection, and contribution to the precipitation development simply doesn't emerge. If such a picture can be developed, it would greatly increase the utility of the paper.

The Results (Section 6) has been reorganized in the new paper to reflect your concerns.

[Minor comments omitted...]

REVIEWER B (Russ Schumacher):

Initial Review:

Reviewer recommendation: Accept with major revisions.

General comments: This study uses numerical simulations to further investigate the Snake Plain Convergence Zone (SPCZ) that has been identified and analyzed in previous works. The primary methods for this analysis are a comparison between a control simulation with high-resolution terrain, and a simulation with slightly smoothed topography. The primary features of the SPCZ appear in both simulations but some of them are weaker in the smoothed-terrain simulation.

The SPCZ is a very interesting phenomenon and it has important local effects on precipitation and winds, and has not been adequately examined in the literature. This manuscript provides some further insight into the processes governing the SPCZ. The manuscript is carefully constructed and well organized, though the writing lacks focus in some areas and the primary conclusions to be reached from the simulations are not entirely clear. There are also some other plausible mechanisms that could be considered. As a result of these concerns, I am recommending major revisions and look forward to seeing a revised version. I believe once the main conclusions are solidified somewhat, this study will make a nice contribution to the literature on orographic circulations.

The reviewer has made several good points that have been addressed in the amended manuscript. The paper has been streamlined and refocused with more emphasis on the narration of the event and cause-effect relationships. The strengths and weaknesses of the model simulations and the initialization required a separate section in the amended paper. A new section of the paper addresses the definition of the SPCZ with a figure from Andretta (2011). I have tied the various sections together to further the narration of this case study and clarify the various

conclusions. These changes should address your needs and concerns. Thank you for the review and your constructive points.

Major comments:

1. One thing that could improve the motivation for the study and the readability of the manuscript could be to provide a bit more justification for the “SMOOTH” simulation. It’s stated in the introduction that the primary motivations are to help forecasters better understand the SPCZ and to improve associated precipitation forecasts. However, this doesn’t necessarily jump out to me that the way to do this is by comparing simulations with differing terrain resolution. However, the study does highlight some potential hypotheses regarding the importance of specific terrain features that are tested in these experiments. Perhaps describing some such hypotheses in the introduction will help better set up the analysis of the simulations. Furthermore, a summary near the end of the key differences between the two simulations might be helpful. From my reading, the take-home message is that the main features of the SPCZ still occur even with smoothed terrain, but that some of the fine-scale features differ slightly.

The reviewer has written some insightful comments here. The SPCZ does develop in both simulations but the middle convergence band (C2) and vorticity belt (P2N2) seem much weaker or absent in the coarse Little Lost River Valley. I have devoted an entire new section in the revised manuscript to explain the need for the CONTROL and SMOOTH simulations.

2. Some of the sections seem perhaps over-emphasized and others not emphasized enough. Section 5e shows that there is some surface-based CAPE during the afternoon in this simulation, but not much discussion is given to this. To me, the simplest hypothesis for enhanced precipitation in the plain is that convergence (from the demonstrated mechanisms) lifts parcels to their LFCs and initiates upright convection. Since there is at least some CAPE that develops in the afternoon, one wonders whether this is what’s happening. It seems that this hypothesis may need to be investigated first (and refuted if it’s not a sufficient explanation) prior to moving on to the other instabilities. It may be that upright convection can explain the main precip band in the plain but not the bands that form in association with the smaller-scale topographic features. Also, is there any elevated CAPE? Finally, there is a lot of discussion of convective/potential instability, and it could be that layer lifting up the terrain is important, but I don’t see why parcel lifting (conditional instability) might not also be occurring.

After an examination of some cross sections, the CAPE is at or close to the surface. Yes, it is probably tied to the diurnal cycle and there is conditional instability near band B3. The convective instability occurs with layer lifting of air up the gentle slope of the Magic Valley. The positive CAPE is east of that area. However, I have removed the CAPE animations from the paper. I have mentioned the parcel instability in the amended paper.

3. The PV discussion in section 5f seems a bit more complicated than it needs to be. Instead of jumping into the discussion of EPV, why not address the convective and inertial instabilities first? They can be explained without bringing up PV. Then, if the idea is that convective/potential symmetric instability is important, then move on to discussing EPV at that point.

After review, I have removed the PV budget analysis entirely and focused efforts on identifying the convective and inertial instabilities. The EPV analysis is presented to show the locations of inertial and convective instability and associations with the topographically-forced reflectivity towers. These sections in the new manuscript have been streamlined or rewritten completely.

[Minor comments omitted...]

Second Review:

Reviewer recommendation: Accept with minor revisions.

General Comments: In the revised manuscript, the organization of the content and the motivation for the study has been improved considerably. Furthermore, some of the more speculative aspects of the original manuscript have been wisely removed. However, there remain some issues with the clarity of some of the explanations as well as a few other minor problems. As a result, I recommend further minor revisions for this manuscript prior to publication.

The amended paper contains the reviewer's recommendations. Thank you for the review.

[Minor comments omitted...]

REVIEWER C (Daniel J. Kirshbaum):**Initial Review:**

Recommendation: Accept with major revisions.

Summary: This manuscript presents a numerical case-study analysis of a winter precipitation event in the Snake River Plain of Idaho, focusing on high-resolution simulations with the WRF model. Simulations with high- and low-resolution terrain are considered. A variety of simulated diagnostics are calculated, followed by hypotheses/speculations as to their potential contribution to the precipitation event. There are some interesting results, mainly that snowbands may form in statically stable regions of locally generated conditional symmetric (and/or inertial) instabilities. Despite the existence of publishable results, I still think that the manuscript needs major work to become publishable, for reasons that are specified below.

Major comments:

1. My main concern with this manuscript is that, with the way it is written, it will have difficulty maintaining a reader's interest. A well written scientific study is told like a story, with analysis that is well motivated and continually builds toward interesting conclusions. It presents plausible hypotheses and evaluates them to hone in on a convincing result. This study, however, is presented as a survey of disconnected analyses, with no roadmap or motivation behind them. Each subsection of section 4 is written as if it is independent from the rest of the paper. There is no learning from previous findings or buildup towards an interesting conclusion, only a variety of pieces that are loosely connected at the end. The lack of motivation or coherent logic gives a reader very little motivation to keep reading. As another example of the lack of motivational material, the author never explains why the both the CONTROL and SMOOTH simulations are performed. There are rather obvious motivations for doing such experiments, but it is the author's job to specify them or else there is no reason for the reader to care about the results.

The reviewer has made several valid points that have been addressed in the amended manuscript. There are studies that do not provide much motivation for reading them and I certainly don't want this paper to fit in that category. Hence, I have reorganized the paper and have added new sections while deleting non-essential figures. The strengths and weaknesses of the model simulations have required a separate section (Section 6b) in the paper. A definition of the SPCZ and associated figure has been provided in the amended text. The motivation for the study has been expanded in Section 1. The narration of the case study has been reorganized in the amended paper with a better coordination among the various sections. These changes will hopefully percolate the reader's interest and provide a better "roadmap". Thank you for the review and constructive feedback.

2. Although animation-friendly electronic journals like this may be the way of the future, one should be wary of relying too much on animations. This paper has a whopping eight of them. It takes a toll on the reader to repeatedly have to work through different external folders and files to see each loop unfold (as I had to do in this case), then cross-reference it against the text. While animations can be helpful at times, I think that due to their inherent inefficiencies they should be used sparingly. There is still some value in the scientific skill of condensing large volumes of data into still figures, tables, or in-line quantities. The author is obliged to filter out extraneous things and focus the presentation on just the most relevant images. I suggest at least halving the number of animations in future versions, replacing the removed ones with one or more snapshots that can be viewed inline (and/or from a printout).

The animations provided a time series of the variables and were never meant to clutter the manuscript but rather to replace numerous inline figures which make the paper unnecessarily incoherent and longer. In the interest of all the reviewer comments and paper length, I have removed the animations for the composite reflectivity, CAPE, and PV budget.

3. Figure 6 dedicates the better part of a page to showing Froude numbers over a large geographic area. Firstly, it is unclear how these are calculated, just saying they are calculated in GEMPAK is not sufficient. An actual method is required, because different methods give strikingly different results. For one thing, U shouldn't be the full wind speed, it is only the cross-barrier component. I don't know whether this was considered in the calculation. Also, given that Fr is a rather loose and poorly defined non-dimensional scaling quantity, presenting its full horizontal distribution is unnecessary. This entire figure could be replaced by one or two inline Fr values representing the background flow upstream of the mountainous region of interest (e.g., somewhere in western Idaho or eastern Washington, depending on the background low-level wind direction).

The GEMPAK methodology for computation of Froude Number (Fr) has been highlighted in the amended paper. The importance and relevance of the Froude values (Fr) plotted at the WRF-ARW model grid points lies in determining the critical aspects of the flow relative to the downstream barrier or the ratio of the kinetic (flow speed) to the potential energy (barrier height). Displaying one or two values of Fr on a map really diminishes a key advantage of using the high resolution gridded model output. I closely followed Mass and Ferber (1990) in calculations of the Froude Number at KBOI and KEGG for the Andretta (2011) dissertation. Mass and Ferber explicitly define U as the average wind speed in the layer over the approximate effective depth of the barrier. Hence, I have left these calculations and figures stand based on the prior research methodology. The model results are consistent with the observations.

4. I don't see the purpose of the movies in Figs. 9 and 12, as well as the entire section 5d (microphysics). These are all showing essentially the same thing that was already evident in Fig. 5 that flow-parallel precipitation bands develop in the valley over the course of the simulation and that the westernmost one is the most intense.

The WRF-ARW microphysics animations show that there are snow and graupel accumulations produced in the western Magic Valley but not all falling out at the ground as surface precipitation because of sublimation (drying) and local subsidence (Andretta 2011). This is one reason the model three-hourly precipitation plots show a smaller westward extension of the precipitation shield versus the KSFY WSR-88D radar derived precipitation.

5. The above comments reflect an interest in streamlining this paper by trimming the redundant and/or unnecessary material. By contrast, there is an interesting (though maybe not entirely new) result shown towards the end (Fig. 14 mainly) that significant snowfall can be produced by bands of inertial instability in the lee of the mountains. In my view, an exposition on the dynamics of those bands (e.g., through horizontal low-level EPV/precipitation plots and

band-parallel vertical cross-sections showing relevant dynamical and microphysical quantities) would be a more profitable use of space than Figs. 9 or 12.

The EPV banners in the Upper Snake River Plain are dominated by horizontal (inertial) (in)stability. Since this term is just absolute vorticity in the source equation, I have already plotted this quantity (Fig. 12: relative vorticity = absolute vorticity - f) earlier in the paper so there is little added value. Based on the WRF-ARW 4-km model simulations documented in Andretta (2011), there is little evidence to suggest that EPV banners originating from horizontal instabilities generate precipitation bands; any spatial correlation is without any physical causation. The three-hour precipitation plots have been included in the paper as part of the model validation. I have constructed several cross sections normal to the snowbands to examine the thermal structure, simulated reflectivity, instabilities, and circulations. These figures should address your concerns.

6. P. 17R, Eq (3): First, there are a variety of symbols in this equation that are never defined. Second, why does this analysis consider the source/sinks of PV, when the previous analysis considered EPV? This is important because, whereas EPV is conserved under diabatic processes, PV isn't. So, if the bands are linked to regions of perturbation EPV, the diabatic source term in (3) is irrelevant to explaining their origin. In other words, (3) isn't necessary in the previous analysis of EPV already revealed that diabatic processes were unimportant to the band generation and their origin must be linked to something else. I am also not sure if I agree with the author's conclusion that, "In sum, friction organizes the convergence bands and vorticity belts during this autumn SPCZ event." I agree that some form of dissipation is generating PV, but it may not be surface friction. Many other mountain dynamical processes can also be responsible for turbulent dissipation (e.g., flow splitting, wave breaking, wake formation, etc.).

The section on the PV budget equation has been removed from the amended paper. As the reviewer points out, since EPV is conserved for diabatic processes then the non-conservation of EPV in the anomalies of the cross sections is tied to frictional dissipation or other causes.

[Minor comments omitted...]

Second Review:

Reviewer recommendation: Accept with major revisions.

This is my second review of a paper to which I originally recommended major revisions. I have read the revised manuscript and find the paper to be improved in multiple ways. In particular, the results section reads better and seems more coherent. Although reduced in number, I still find the time-lapse movies quite cumbersome to deal with (they do not load automatically from the .docx file so I have to find and play them myself), but that might just be me so I will live with it and let the readership be the judge. But I found that my major comments 3 and 5, so I restate them and a couple others here and try to better explain my points. I also give fairly prescriptive suggestions for how to address some of them.

The amended paper contains the reviewer's recommendations. Thank you for the review.

Major comments:

1. My major comment 3 before involved the Froude-number analysis. The author has now provided a description of the calculation (which I appreciate), as well as some GEMPAK code within the text (I address my view of the GEMPAK code below). Based on the explanation, I'm not sure if the author has calculated Fr correctly. The winds used are the full winds (averaged over a layer), when really they should be the component of winds across a topographic feature of interest.

I think it's a waste of space to make Fr a 2D field—it is most commonly a scalar representing the potential for upstream flow (with fixed U and N) to surmount a barrier (with fixed H). This is because the standard derivation of Fr assumes a well-defined large-scale flow, so that the perturbations induced by the terrain (which can extend far upwind and downwind of the terrain itself) can be scaled against it. A 2D field of Fr mixes up the large-scale and the perturbed flow, leaving the relevance questionable and the interpretation difficult. The author now provides point values of Fr at a couple locations, and I think that's sufficient. The topographic smoothing between the two simulations don't have much of an impact on the overall flow regime (which Fr is meant to diagnose).

The large scale flow is perturbed by the interaction with the barrier. The lower to mid-level flow direction is NW-W and roughly normal to the barrier (e.g., Central Mountains). The reviewer claims that the Froude number is incorrectly computed and yet does not provide an alternative methodology. In defense of my work in this paper and the dissertation, I cited Mass and Ferber (1990) for the general methodology. The 2D Froude Number plot is relevant, providing a spatial estimate of the flow blocking by the Central Mountains. The values of Fr are clearly lower on the northwest and western sides of the barrier relative to the southern side, as verified by the KGEK and KBOI soundings. The model results are validated by these observations. Moreover, this blocking is clearly reduced in the SMOOTH run. Those are/were the main points.

2. In his response to my comment 5, the author has left me confused. The response definitively says that the inertially unstable PV banners play no role in triggering convection. Yet the conclusion says, “The numerical simulations indicated that several topographically-generated snowbands occurred in the presence of conditional, convective, and inertial instabilities,” and that “Inertial instability formed within the anticyclonic (negative) vorticity belts and near some snowbands in the Upper Snake River Plain.” Since these banners are the only source of inertial instability (see Fig. 6), these statements imply that the banners are indeed important for the snowbands. If they aren't important, shouldn't that point be made (and defended) in the paper? Also, if these bands aren't developing from inertial, symmetric, or convective instability, then what process is causing them?

This paper has described topographically-forced convergence (convection) in the Snake River Plain. That is the main forcing mechanism (forced convection) for the precipitation bands. There are instabilities present, e.g., near band B3 (free convection) which locally enhanced precipitation in the Arco Desert. I never disputed that. Inertial instability exists but it is unclear how horizontal instabilities lead to vertical motions and spatial correlations with snowbands do not imply direct physical causations. I stated that very clearly in the paper. To fully address this concern, I have qualified the amended text regarding the importance of the various instabilities relative to the principal forcing mechanism (terrain). We can agree that this topic needs further study and more modeling work on other SPCZ cases (at a later time).

3. Some of the new text added to the paper reads awkwardly. First, all of the GEMPAK code in section 5 should be removed. I have never seen anything like that in a paper before. The author should be able to explain the methodology in words, even if the algorithm was created by somebody else. The reader just needs the physical procedure, not the code (note that only a small fraction of the community, particularly those outside the US, knows about GEMPAK anyway).

Second, I find it surprising that section 1b is entitled “Description of hypotheses” but it only talks about research questions. Questions and hypotheses are different things.

I provided the equations because several of the reviewers wanted an explanation of the calculations appearing in the figures. The GEMPAK code has been removed from the amended paper and a qualitative description provided in place of it. Research questions form the basis for hypotheses. Since this is a major issue, I have rephrased Section 1b to read: “Description of Research Questions”.

Third, the entire first paragraph of section 3 could be replaced with a sentence: “Based on the characteristic flow speeds and length scales during SPCZ events, the Rossby number ($Ro = U/fL$, where U and L are characteristic flow speed and length scale and f is the Coriolis parameter) is often around unity, implying highly ageostrophic flow.” Then, in the next paragraph the author essentially redefines ageostrophic flow. The text needs to be more concise. I suggest removing the first paragraph of this section and merging the Rossby-number discussion into the text on the PGF and Coriolis forces.

This suggestion is a valid point; both discussions describe alternate definitions of the ageostrophic flow. Hence, these sections have been reorganized in the amended paper. After further review, two to three paragraphs are more appropriate and less cumbersome for the reader.

Fourth, at various places the text says something similar to, “[The SPCZ] consists of leeward and windward flow regimes under low Froude number (stable blocked flow) in a post cold-frontal environment.” The term “windward and leeward flow regimes” is quite confusing and difficult to imagine. Windward and leeward are not “flow regimes”—they are the sides of a barrier.

I explained (at great length) the meaning of the flow regimes in Section 3 with Figure 2. Why and how is it unclear? Both flow regimes are characteristics of sides of the topographic barriers (Southern Highlands: upslope-windward side) and (Central Mountains: leeward side).

4. Although the time-lapse plots weren't my favorite, I think the removal of the CAPE plot altogether does more harm than good. I don't think an animation of CAPE for the entire event is needed, but a representative snapshot wouldn't hurt. Ideally, the reader would have a picture of the CAPE, symmetric instability, and inertial instability at a time when (or just before) multiple snowbands were active. This would explain the instabilities giving rise to the bands.

To address this issue, the CAPE animation has been reinserted into the amended paper.